

1 **Reduced histone gene copy number disrupts *Drosophila* Polycomb function**

2

3 Jeanne-Marie E. McPherson^{1,3}, Lucy C. Grossmann², Robin L. Armstrong^{1,3}, Esther
4 Kwon², Harmony R. Salzler^{2,3}, A. Gregory Matera¹⁻⁵, Daniel J. McKay^{1-4*}, Robert J.
5 Duronio^{1-5*}

6

7 ¹Curriculum in Genetics and Molecular Biology, University of North Carolina, Chapel Hill,
8 NC, 27599 USA

9 ²Department of Biology, University of North Carolina, Chapel Hill, NC, 27599, USA

10 ³Integrative Program for Biological and Genome Sciences, University of North Carolina,
11 Chapel Hill, NC, 27599, USA

12 ⁴Department of Genetics, University of North Carolina, Chapel Hill, NC, 27599, USA

13 ⁵Lineberger Comprehensive Cancer Center, University of North Carolina, Chapel Hill, NC,
14 27599, USA

15 *Corresponding author: Integrative Program for Biological and Genome Sciences,
16 University of North Carolina, Chapel Hill, NC, 27599 USA. Email: duronio@med.unc.edu

17 *Corresponding author: Integrative Program for Biological and Genome Sciences,
18 University of North Carolina, Chapel Hill, NC, 27599 USA. Email:
19 dmckay1@email.unc.edu

20 **Keywords:** *Drosophila melanogaster*; chromatin; development; canonical histone; variant
21 histone; Polycomb

22

23

24

25

26

27

28

29

30

31

32

33

34 **Abstract**

35 The chromatin of animal cells contains two types of histones: canonical histones that are
36 expressed during S phase of the cell cycle to package the newly replicated genome, and
37 variant histones with specialized functions that are expressed throughout the cell cycle
38 and in non-proliferating cells. Determining whether and how canonical and variant
39 histones cooperate to regulate genome function is integral to understanding how
40 chromatin-based processes affect normal and pathological development. Here, we
41 demonstrate that variant histone H3.3 is essential for *Drosophila* development only when
42 canonical histone gene copy number is reduced, suggesting that coordination between
43 canonical *H3.2* and variant *H3.3* expression is necessary to provide sufficient H3 protein
44 for normal genome function. To identify genes that depend upon, or are involved in, this
45 coordinate regulation we screened for heterozygous chromosome 3 deficiencies that
46 impair development of flies bearing reduced *H3.2* and *H3.3* gene copy number. We
47 identified two regions of chromosome 3 that conferred this phenotype, one of which
48 contains the *Polycomb* gene, which is necessary for establishing domains of facultative
49 chromatin that repress master regulator genes during development. We further found that
50 reduction in *Polycomb* dosage decreases viability of animals with no *H3.3* gene copies.
51 Moreover, heterozygous *Polycomb* mutations result in de-repression of the Polycomb
52 target gene *Ubx* and cause ectopic sex combs when either canonical or variant *H3* gene
53 copy number is also reduced. We conclude that Polycomb-mediated facultative
54 heterochromatin function is compromised when canonical and variant *H3* gene copy
55 number falls below a critical threshold.

56 **Introduction**

57 To control access to information encoded in the genome, eukaryotes organize their DNA
58 into chromatin, which regulates all DNA-dependent processes including transcription,
59 DNA replication, and DNA damage repair (Allis CD 2007; Kornberg and Lorch 2020). The
60 fundamental unit of chromatin is a nucleosome composed of approximately 150 bp of
61 DNA wrapped around a histone octamer containing two copies of each of the four core
62 histones: H2A, H2B, H3, and H4 (Luger et al. 1997). Tight control over histone levels is
63 essential for normal genome function. For instance, mutations in *abo* and *mute*—which
64 negatively regulate histone mRNA levels—reduce viability in *Drosophila melanogaster*
65 (Berloco et al. 2001; Bulchand et al. 2010). In budding yeast, mutations that cause an
66 accumulation of excess histone proteins result in impaired growth, DNA damage
67 sensitivity, and chromosome loss (Meeks-Wagner and Hartwell 1986; Gunjan and
68 Verreault 2003). Conversely, conditional repression of histone transcription during S
69 phase impairs DNA replication and causes cell cycle arrest in yeast and fruit flies (Han et
70 al. 1987; Sullivan et al. 2001; Gossett and Lieb 2012). Similarly, deletion of all *D.*
71 *melanogaster* canonical histone genes leads to cell cycle arrest and embryonic lethality
72 (Smith et al. 1993; Günesdogan et al. 2010; McKay et al. 2015). Histone chaperone
73 mutations that reduce incorporation of histone proteins into chromatin cause spurious
74 transcription, chromosome segregation defects, chromosomal rearrangements, and
75 enhanced DNA damage (Clark-Adams et al. 1988; Nelson et al. 2002; Myung et al. 2003;
76 Ye et al. 2003; Nashun et al. 2015; Mühlen et al. 2023a). For these reasons, precise

77 regulation of histone mRNA and protein levels is critical for normal cell function and
78 development, yet we have an incomplete understanding of the mechanisms involved.

79 Most research investigating the mechanisms of histone expression has focused
80 on the canonical histone genes, which are synthesized in large amounts during S phase
81 to properly package newly replicated DNA into chromatin. This work provides evidence
82 supporting regulation at both the transcriptional and post-transcriptional levels (Marzluff
83 and Duronio 2002; Duronio and Marzluff 2017). For example, in Chinese hamster ovary
84 cells, canonical histone mRNA levels increase 35-fold as cells enter S phase (Harris et
85 al. 1991). As cells exit S phase, canonical histone transcription is terminated and the
86 corresponding mRNAs are rapidly degraded (Kaygun and Marzluff 2005; Eriksson et al.
87 2012). Coordinate expression among histone genes to maintain nucleosome subunit
88 stoichiometry is also important; this requirement is reflected in the clustered arrangement
89 and co-regulation of the canonical histone genes in multiple species, including *D.*
90 *melanogaster*, yeast, and mammals (Lifton et al. 1977; Smith and Murray 1983; Eriksson
91 et al. 2012). In the *D. melanogaster* histone gene complex (HisC, see **Figure 1A**), *H2A*
92 and *H2B* share a bidirectional promoter, as do *H3* and *H4* (Lifton et al. 1977). Histone
93 protein levels are also controlled post-translationally. For example, yeast histones that
94 are not chromatin-bound are rapidly degraded, suggesting that excess histone proteins
95 are deleterious to cell function (Singh et al. 2009). Moreover, during *Drosophila* oogenesis
96 H2Av protein levels are regulated by Jabba, which binds H2Av and prevents degradation
97 of excess histones (Stephenson et al. 2021).

98 Whereas canonical histones are encoded by multiple genes that are expressed
99 exclusively during S phase of the cell cycle (**Figure 1A, 1B**), an additional layer of
100 complexity is provided by the expression of cell cycle independent histones (Franklin and
101 Zweidler 1977; Verreault et al. 1996; Marzluff et al. 2002; Tagami et al. 2004). These so-
102 called ‘variant’ histones are typically encoded by one or two genes and are expressed
103 throughout the cell cycle (**Figure 1A, 1B**) (Urban and Zweidler 1983; Pantazis and Bonner
104 1984; Zweidler 1984; Brown et al. 1985; Piña and Suau 1987; Wunsch and Lough 1987;
105 McKittrick et al. 2004; Tagami et al. 2004; Mito et al. 2005; Szenker et al. 2011; Maze et
106 al. 2015; Tvardovskiy et al. 2017; Sauer et al. 2018). The tight control of canonical histone
107 levels and the severe negative impact of histone mis-expression raises the possibility that
108 coordinate regulation between canonical and variant histones is important for genome
109 function and stability. For instance, in the early *Drosophila* embryo an increase in the ratio
110 of variant H2Av to canonical H2A causes mitotic defects and reduces viability (Li et al.
111 2014). Here, we address the question of coordinate regulation between variant and
112 canonical histone genes by focusing on those encoding histone H3.

113 In *D. melanogaster*, the non-centromeric H3 variant is encoded by two genes that
114 produce identical proteins, *H3.3A* and *H3.3B*. (**Figure 1A**). Variant H3.3 differs from
115 canonical H3.2 by only four amino acid residues, and these differences are highly
116 conserved among other animals including humans (Malik and Henikoff 2003; Szenker et
117 al. 2011) (**Figure 1C**). Three of the four residues are found in the globular domain and
118 are known to modulate interactions with the histone chaperone complexes that deposit
119 histones into chromatin (Grover et al. 2018). Canonical H3.2 is deposited during DNA
120 replication by CAF-1 (chromatin assembly complex 1) (Smith and Stillman 1989;
121 Verreault et al. 1996; Shibahara and Stillman 1999; Tagami et al. 2004; Sauer et al. 2018).

122 Variant H3.3 is deposited into chromatin by the ATRX (alpha-thalassemia X-linked mental
123 retardation protein) complex and the HIRA (histone cell cycle regulator) complex (Ahmad
124 and Henikoff 2002; Tagami et al. 2004; Schneiderman et al. 2009; Goldberg et al. 2010;
125 Lewis et al. 2010; Rai et al. 2011; Orsi et al. 2013; Ray-Gallet et al. 2018; Torné et al.
126 2020). Whereas H3.2 is deposited evenly genome-wide during replication, H3.3 is
127 enriched at sites with high nucleosome turnover, including active regulatory elements,
128 transcribed gene bodies, and pericentromeric regions (Ahmad and Henikoff 2002;
129 McKittrick et al. 2004; Mito et al. 2005; Wirbelauer et al. 2005; Loyola and Almouzni 2007;
130 Goldberg et al. 2010; Szenker et al. 2011; Martire and Banaszynski 2020 Jul 14). The
131 fourth amino acid difference between H3.2 and H3.3 occurs at position 31 in the post-
132 translationally modified N-terminal tail (Szenker et al. 2011). Position 31 is an alanine in
133 H3.2 (H3.2A31) and a serine in H3.3 (H3.3S31), which can be phosphorylated (Hake et
134 al. 2005; Armache et al. 2019; Martire et al. 2019; Sitbon et al. 2020). Other residues on
135 the N-terminal tails of H3.2 and H3.3 are also differentially enriched in post-translational
136 modifications (PTMs), likely due to their differential localization in the genome. Relative
137 to H3.2, H3.3 is enriched with PTMs associated with active chromatin (e.g. H3K4me3)
138 and depleted in marks associated with inactive chromatin (e.g. H3K9me2) (McKittrick et
139 al. 2004; Hödl and Basler 2012). Although the mechanisms regulating canonical and
140 variant histone mRNA and protein levels are distinct, we do not know if and how these
141 mechanisms are coordinated to supply the necessary amount of each histone isotype
142 across the genome. Here we use *D. melanogaster* to explore this question by examining
143 the consequences of manipulating the relative number of canonical and variant *H3* genes.

144 Genetically manipulating histone gene copy number is challenging in many
145 metazoans, including mice and humans, because canonical histones are encoded by
146 multiple gene clusters located at distinct chromosomal locations (Marzluff et al. 2002b).
147 *D. melanogaster* is a powerful organism to investigate the effects of altering histone gene
148 copy number because all ~100 haploid copies of the canonical histone genes are
149 tandemly repeated (**Figure 1A**) and can be removed with a single genetic deletion, $\Delta HisC$
150 (Günesdogan et al. 2010). The ability to manipulate histone genes in *D. melanogaster* led
151 to the discovery that canonical histone gene copy number is a modifier of position effect
152 variegation (PEV), a genetic phenomenon associated with heterochromatin.
153 Heterozygosity of the histone locus results in suppression of PEV, suggesting that histone
154 abundance contributes to maintenance of epigenetic silencing of H3K9me3-marked
155 constitutive heterochromatin (Moore et al. 1979; Moore et al. 1983; Sinclair et al. 1983).
156 The ability to manipulate histone gene copy number in *D. melanogaster* has been
157 extended in recent years. Replacement of all ~200 copies ($200xWT$) of the canonical
158 histone genes with a transgene containing 12 wild-type canonical histone gene repeat
159 units ($12xHWT$, see **Figure 1A**) is sufficient to support development and provides a
160 means of altering canonical histone gene copy number with precision (McKay et al. 2015).

161 Here, we report that $12xHWT$ viability depends on expression of variant *H3.3*
162 genes, whereas $200xWT$ viability does not. This finding suggests that coordination of
163 H3.2 and H3.3 protein levels is necessary for proper development when either *H3.2* or
164 *H3.3* gene copy number is reduced. We conducted a screen to identify genes involved in
165 the coordinated control of *H3.2* and *H3.3*. We identified a deficiency that uncovers *Yem*,
166 a component of the HIRA histone chaperone complex, the function of which may be
167 particularly important when *H3.2* gene copy number is reduced. Surprisingly, we also

168 found that reduction of *Polycomb* (*Pc*) gene function decreases viability of flies that have
169 reduced numbers of *H3.3* genes. Furthermore, we found that reductions in either *H3.2* or
170 *H3.3* gene copy number disrupts Polycomb-mediated gene repression. Rather than *Pc*
171 being involved in the coordinate expression of canonical and variant H3, we conclude
172 from these findings that the appropriate balance of *H3.2* and *H3.3* genes is critical for the
173 proper epigenetic silencing of developmental genes and maintenance of facultative
174 heterochromatin function.

175 **Results**

176 ***H3.3* is required for viability when *H3.2* gene copy number is reduced.**

177 To examine whether coordination between canonical *H3.2* and variant *H3.3* gene
178 expression contributes to *Drosophila* development, we measured the effects of altering
179 the relative number of canonical versus variant histone gene copies on viability and
180 fertility. Zygotes lacking all canonical histone genes ($\Delta HisC$) arrest early in embryonic
181 development, and this lethality can be rescued with a transgene encoding 12 tandemly
182 arrayed histone gene repeats (*12xHWT*), providing an opportunity to manipulate
183 canonical histone gene dose over an ~18-fold range (**Figure 1A, Figure 1D**) (McKay et
184 al. 2015). Null mutations of either *H3.3A* or *H3.3B* have no effect on viability or fertility of
185 flies containing the normal complement of canonical histone genes, but only 50% of the
186 expected number of *H3.3A*, *H3.3B* double mutants (*H3.3^A; 200xWT*) eclose as adult flies,
187 which are infertile (**Figure 1D, Figure 1 in File S1**) (Sakai et al. 2009). *H3.3^A* animals
188 heterozygous for a *HisC* deletion (*H3.3^A; 100xWT*) survive to adulthood at a similar
189 frequency as *H3.3^A; 200xWT* animals (54.2% and 50% of expected, respectively) (**Figure**
190 **1D**). However, reducing canonical histone gene copy number to 20 (*H3.3^A; 20xWT*)
191 results in only 17.1% of the expected number of adults (**Figure 1D**). A further reduction
192 to 12 histone gene repeats (*H3.3^A; 12xHWT*) results in a complete loss of viability of flies
193 lacking variant *H3.3* genes (**Figure 1D**). *H3.3^A; 12xHWT* lethality is rescued by one copy
194 of either *H3.3A* or *H3.3B*, and the adults of these genotypes are fertile (**Figure 1D, Figure**
195 **1 in File S1**). Thus, we conclude that *H3.3* expression is necessary for completion of
196 development when canonical histone gene copy number is reduced to 12, and that the
197 probability of animals lacking *H3.3* to complete development increases with increasing
198 numbers of canonical histone genes. Furthermore, our data support previous
199 observations that *H3.3* is required for male and female fertility (**Figure 1D**) (Sakai et al.
200 2009). Collectively, these data suggest that *H3.3* compensates for reduced *H3.2* gene
201 copy number to maintain a critical threshold of total H3 protein.

202 ***H3.3* mRNA and protein levels do not change when *H3.2* gene copy number is** 203 **reduced.**

204 Mechanisms that compensate for altered variant versus canonical histone genes could
205 operate at many levels, including transcription, translation, histone deposition into
206 chromatin, or histone protein turnover. For instance, increased *H3.3* expression could
207 compensate for reduced *H3.2* gene copy number, potentially explaining why *12xHWT*
208 animals do not survive in the absence of *H3.3* genes. We reasoned that measuring
209 steady-state mRNA and protein levels could reveal evidence of such compensatory
210 mechanisms. To determine whether *H3.3* steady-state mRNA levels are elevated in
211 *12xHWT* animals, we compared *H3.3* mRNA levels in *12xHWT* versus *200xWT* control

212 animals in an RNA-sequencing data set obtained from third instar larval brains. We found
213 no significant difference in *H3.3A* or *H3.3B* mRNA levels in *12xHWT* compared to
214 *200xWT* cells (**Figure 2A**). Consistent with these RNA-seq data, immunoblots of third
215 instar larval wing imaginal discs show comparable levels of H3.3 protein in *12xHWT* and
216 *200xWT* controls (**Figure 2B**). We conclude that compensation for reduced *H3.2* gene
217 copy number in *12xHWT* animals does not occur via changes in the steady-state levels
218 of *H3.3* mRNA or protein, as measured by RNA-sequencing or immunoblotting.

219 We considered the possibility that expression of *H3.2* becomes uncoupled from S
220 phase upon loss of *H3.3*, thereby maintaining a pool of H3 outside of S phase even when
221 *H3.3* genes are absent. To determine whether *H3.2* transcripts are present in cells outside
222 of S phase in the absence of *H3.3* genes, we combined EdU staining with RNA-FISH in
223 the developing eye of *200xWT*, *H3.3^A*, *H3.3^A*; *12xHWT*, and *12xHWT* animals. We
224 observed that *H3.2* mRNA is only detected in EdU positive cells in all four genotypes,
225 indicating that *H3.2* transcription is not uncoupled from S phase when *H3.2* and/or *H3.3*
226 gene copy number are reduced (**Figure 2C**).

227 **A genetic screen for genes sensitive to reduced histone H3 gene copy number.**

228 The inability to detect evidence of histone gene coordination at the molecular level
229 motivated us to instead take an unbiased genetic approach. Performing a screen in a
230 genotype with reduced variant and canonical histone gene copy number could potentially
231 identify genes that (i) regulate histone gene expression, (ii) coordinate expression
232 between variant and canonical histone genes, or (iii) are otherwise sensitive to reduced
233 histone levels. As described above, *12xHWT* animals are viable and fertile at wild-type
234 frequencies (**Figure 1D**); however, *H3.3^A*; *12xHWT* flies are inviable (**Figure 1D**). We
235 therefore reasoned that we could identify other genes that when mutated would reduce
236 the viability of *12xHWT* animals. Because having one copy of *H3.3A* or *H3.3B* is sufficient
237 to retain viability in a *12xHWT* background (**Figure 1D**), we decided to screen using a
238 *12xHWT* background that is further sensitized by the removal of both copies of *H3.3A*.
239 We refer to this genotype as *H3.3A^A*; *12xHWT* (**Figure 3A**).

240 First, we conducted a proof of principle screen using single gene loss of function
241 alleles or deficiencies covering genes with potential roles in histone function. We tested
242 histone H3 chaperones (e.g. *Asf1*, *Yem*, *Xnp*), cell cycle regulators (e.g. *E2F*, *Stg*), and
243 genes involved in the control of histone mRNA synthesis or chromatin regulation (e.g.
244 *Slbp*, *wge*, *Arts*, *Dre4*). We performed crosses that produced *H3.3A^A*; *12xHWT* progeny
245 heterozygous for individual mutations or deficiencies and determined whether the
246 progeny had reduced or increased viability compared to *H3.3A^A*; *12xHWT* control siblings.
247 Of the 23 mutations tested, heterozygosity of three deficiency mutations—*Df(3R)BSC874*
248 (*Df 66*), *Df(3R)BSC500* (*Df 67*), and *Df(3R)BSC501* (*Df 68*)—resulted in a significant
249 reduction in viability of *H3.3A^A*; *12xHWT* flies compared to control siblings, with only 8.4%,
250 57.9%, and 77.6% of expected surviving to adulthood, respectively (**Figure 3B**, **Table 1**).
251 Interestingly, three other deficiencies *Df(3R)ro80b* (81), *Df(3R)BSC527* (*Df 82*), and
252 *Df(3R)Exel6210* (*Df 83*) resulted in a significant increase in viability of *H3.3A^A*; *12xHWT*
253 flies compared to control siblings, but we did not pursue these further (**Figure 3B**, **Table**
254 **1**). Notably, the three deficiencies that reduce *H3.3A^A*; *12xHWT* viability overlap the same
255 76.6 kb region on chromosome 3R (chr3R) (**Figure 3C**). To further define the genomic
256 region responsible for the genetic interaction, we tested three other deficiency mutations

257 that overlap this region. *Df(3R)BSC789* (Df 70), *Df(3R)ED6310* (Df 72), and Df 83, which
258 overlap other regions of Df 66, Df 67, and Df 68, did not result in a significant reduction in
259 viability. Therefore, the region of interest is limited to a 26.4 kb region defined by the left
260 breakpoints of Df 67 and Df 72 at genomic positions 98F10 and 98F12 (**Figure 3C**).
261 Seven annotated genes reside within this region of interest: *Alg13*, *Atg14*, *dgt6*, *Ctl2*,
262 *Pdhb*, *Vha100-1*, and *yem*, an H3.3 specific chaperone (**Figure 3C**). Thus, one possible
263 explanation for these genetic results is that heterozygosity of *yem* attenuates
264 incorporation of H3.3 protein (derived from the *H3.3B* locus) into chromatin enough to
265 reduce the viability of *H3.3A^A; 12xHWT* flies. This targeted screen confirms that our
266 genetic paradigm can identify mutant loci that when hemizygous cause sensitivity to a
267 reduction in *H3.2* and *H3.3* gene copy number.

268 To expand our search for such loci, we screened the left arm of chromosome 3
269 (chr3L) using the Bloomington Stock Center Chr3L Deficiency Kit, which consists of 77
270 stocks that cover 97.1% of the chr3L euchromatic genome (**chr3L Df kit stocks in File**
271 **S1**) (Cook et al. 2012; Roote and Russell 2012). Fourteen of the deficiency mutations
272 were excluded from the screen because they carry a mini-white genetic marker, resulting
273 in an eye color that precludes identifying all progeny classes (**chr3L Df kit stocks in File**
274 **S1**). Three additional deficiency mutations were not scored because the crosses failed
275 (**chr3L Df kit stocks in File S1**). Of the remaining 60 deficiency mutations, two resulted
276 in an increase in viability when heterozygous in *H3.3A^A; 12xHWT* flies (**Fig 4A, Table 2**),
277 which we did not pursue further. By contrast, heterozygosity of eleven deficiencies caused
278 significant reductions in viability of *H3.3A^A; 12xHWT* flies (**Figure 4A, Table 2**). Four of
279 these deficiencies (Df 1, 4, 8, and 15, **Figure 4A**) also caused a significant reduction in
280 viability of siblings with one copy of *H3.3A* and 112 copies of the canonical histone genes
281 (*H3.3A^{+/-}; 112xHWT*), suggesting haploinsufficiency. We did not pursue these hits further.
282 Interestingly, of the remaining hits *Df(3L)BSC435* (Df 2) and *Df(3L)BSC419* (Df 3) overlap
283 the same 300 kb region of chr3L (**Figure 4B**). To map the genetic interaction in greater
284 detail, we obtained two additional deficiencies—*Df(3L)BSC418* (Df 52) and
285 *Df(3L)BSC836* (Df 36)—that overlap this same region of chr3L and observed no changes
286 in viability of *H3.3A^A; 12xHWT* flies compared to control siblings (**Figure 4A-B**). Therefore,
287 the genomic region spanning 77.76 kb on chr3L between cytological positions 78C6 and
288 78C8 impairs viability of flies with reduced *H3.3* and *H3* gene copy number.

289 **Histone *H3* gene copy number is a modifier of *Pc* function.**

290 Nine annotated genes reside within the defined genomic interval: *CG12971*, *CG32436*,
291 *CG32437*, *CG32440*, *ebd2*, *Pc*, *Rab26*, *Tbc1d8-9*, and *Tsr1* (**Figure 4B**). To determine
292 which of these genes contributes to viability of flies with reduced histone gene copy
293 number, we generated *H3.3A^A; 12xHWT* animals heterozygous for single gene mutations.
294 *CG12971*, *CG32437*, and *CG32440* were not tested because no loss-of-function alleles
295 exist. Heterozygous MiMIC transposon insertion alleles of *ebd2*, *Rab26*, *Tbc1d8-9*, *Tsr1*,
296 and *CG32436* did not impact viability of *H3.3A^A; 12xHWT* flies (**Figure 4C**). However,
297 three independent alleles of the *Polycomb* gene—*Pc¹*, *Pc³* and *Pc¹⁵*—resulted in
298 significant reductions in viability of *H3.3A^A; 12xHWT* flies (55.0%, 61.8% and 52.4% of
299 expected survive to adulthood, respectively) (**Figure 4C**). These data suggest that
300 *H3.3A^A; 12xHWT* flies are less viable when Polycomb function is reduced.

301 Polycomb group genes encode evolutionarily conserved regulators of cell identity.
302 Polycomb complexes function to heritably silence expression of master regulator genes,
303 including the Hox genes, which specify segmental identity (Kassis et al. 2017). In adult
304 males, reduction of Polycomb function can result in homeotic transformations whereby
305 the second (T2) and third (T3) thoracic legs acquire morphological features normally
306 found only on the first thoracic legs (T1). This is most notably manifest by the appearance
307 of sex combs on T2 and T3 legs, which normally only occur on T1 legs (Kaufman et al.
308 1980; Pattatucci et al. 1991). Based on our identification of the *Pc* gene in our genetic
309 screen, we hypothesized that reduced histone gene copy number compromises
310 Polycomb complex function. A prediction of this hypothesis is that reduced histone gene
311 copy number would enhance *Polycomb* mutant phenotypes. Therefore, we evaluated the
312 frequency and severity of homeotic transformations in *H3.3A^Δ; 12xHWT; Pc/+* animals.
313 We observed that *H3.3A^Δ; 12xHWT* males heterozygous for a *Pc* null mutation (*H3.3A^Δ;*
314 *12xHWT; Pc^{3/+}*) exhibit an increased frequency of ectopic sex combs (100%) on T2 and
315 T3 legs relative to *Pc^{3/+}* (48%) or *H3.3A^Δ; 12xHWT* males (0%) (**Figure 5A, Table 3**).
316 Moreover, the expressivity of the ectopic sex comb phenotype is more severe in *H3.3A^Δ;*
317 *12xHWT; Pc^{3/+}* animals relative to *Pc^{3/+}* controls, often having a full set of sex combs on
318 T2 and T3 legs. Males and females of these genotypes also exhibit defects in posterior
319 wing morphology, suggesting partial wing to haltere transformation due to a failure to
320 maintain proper repression of *Ubx* in the wing (**Figure 5C**). Consistent with this
321 hypothesis, immunostaining of *H3.3A^Δ; 12xHWT; Pc^{15/+}* third instar imaginal wing discs
322 revealed ectopic *Ubx* expression in the pouch region (**Figure 5B**). We conclude that
323 histone *H3* gene copy number contributes to Polycomb function during development.

324 Next, we determined whether mutations in other Polycomb group genes cause
325 effects similar to mutations of *Pc* when histone *H3* gene copy number is reduced. *H3.3A^Δ;*
326 *12xHWT* flies heterozygous for null mutations in *Sce* and *Ph*, which encode members of
327 Polycomb Repressive Complex 1 (PRC1), are viable at expected frequencies (**Figure**
328 **5D**). Similarly, heterozygous mutations in Polycomb Repressive Complex 2 (PRC2)
329 genes, *E(z)* and *Su(z)12*, do not cause reductions in viability (**Figure 5D**). *Pc* is a core
330 component of PRC1, suggesting that the function of this Polycomb complex component
331 is particularly sensitive to histone *H3.2* and *H3.3* gene copy number.

332 **Histone *H3.2* and *H3.3* gene copy number are each critical for Polycomb-mediated** 333 **gene silencing.**

334 Since both *H3.2* and *H3.3* gene copy number are reduced in *H3.3A^Δ; 12xHWT* animals,
335 we next determined the individual requirement of either *H3.2* or *H3.3* gene copy number
336 in Polycomb-mediated silencing. We quantified viability and assessed whether Polycomb
337 target genes were de-repressed in either *12xHWT* or *H3.3^Δ* animals that were also
338 heterozygous for a *Pc* null mutation (*12xHWT; Pc^{3/+}* and *H3.3^Δ; Pc^{3/+}*, respectively).
339 *12xHWT; Pc^{3/+}* animals are viable at expected frequencies but have an increased
340 frequency of ectopic sex combs on T2 and T3 legs like *H3.3A^Δ; Pc^{3/+}; 12xHWT* animals.
341 *12xHWT; Pc^{3/+}* animals also exhibit ectopic *Ubx* expression in the wing pouch of third
342 instar imaginal discs and defects in adult posterior wing morphology (**Table 3, Figure 6A-**
343 **D**). *112xHWT; Pc^{3/+}* animals are viable at the expected frequency but also exhibit
344 increased frequencies of ectopic sex combs on T2 and T3 legs relative to *Pc^{3/+}* controls
345 (**Table 3**). Of note, the frequency of ectopic sex combs in *112xHWT; Pc^{3/+}* animals (80%)

346 is significantly lower than *12xHWT*; *Pc*^{3/+} animals (100%) (**Table 3**). Thus, reducing *H3.2*
347 gene dose makes animals sensitive to reduced Polycomb function, and the severity of
348 homeotic transformation is proportional to canonical histone gene copy number. We also
349 found that normal *H3.3* gene dose is necessary for Polycomb function. *H3.3*^Δ; *Pc*^{3/+}
350 animals are not fully viable, with only 59.6% of expected surviving to adulthood (**Figure**
351 **6A**). *H3.3*^Δ; *Pc*^{3/+} males also exhibit increased frequencies of ectopic sex combs on T2
352 and T3 legs (100%), defects in adult posterior wing morphology, and *Ubx* de-repression
353 in the wing pouch of third instar imaginal wing discs (**Figure 6B-D, Table 3**). Animals with
354 one or two copies of *H3.3* survive to adulthood at a similar frequency—79.7% and 77.6%
355 of expected, respectively—and animals with three copies of *H3.3* are viable at the
356 expected frequency (**Figure 6A**). Consistent with these observations, males with only one
357 copy of *H3.3B* also exhibit ectopic sex combs on T2 and T3 legs (**Table 3**). Taken
358 together, these findings indicate that both *H3.2* and *H3.3* gene copy number are
359 independently important for Polycomb-mediated epigenetic silencing, but viability is only
360 affected by reduction in *H3.3* gene copy number.

361 **Discussion**

362 In this study we found that reducing either canonical or variant histone *H3* gene copy
363 number disrupts Polycomb-mediated gene repression. Two major protein complexes
364 establish and maintain Polycomb-mediated repression: Polycomb Repressive Complex 1
365 and 2 (PRC1 and PRC2). PRC2 catalyzes H3K27me₃, both PRC2 and PRC1 bind to
366 H3K27me₃, and PRC1 facilitates repression of local chromatin (Blackledge and Klose
367 2021). Mutations in core components of PRC1 and PRC2 disrupt the formation of these
368 domains and cause transcriptional de-repression of Polycomb targets, such as Hox genes
369 (Kennison and Tamkunt 1988; Paro 1990; Orlando 2003). We found that reduction in
370 canonical or variant *H3* gene copy number results in homeotic transformations associated
371 with de-repression of the Polycomb target genes *Ubx* (posterior wing transformation) and
372 *Scr* (ectopic sex comb development in males). Consistent with these findings, a previous
373 study in *D. melanogaster* found that heterozygosity of *HisC* suppresses homeotic
374 transformation phenotypes in animals with a mutation that causes ectopic silencing of
375 Polycomb target genes (Bajusz et al. 2001). Reduction of canonical histone gene copy
376 number in *D. melanogaster* also modifies position-effect variegation, a phenomenon
377 mediated by H3K9me₃-marked constitutive heterochromatin (Moore et al. 1979; Moore
378 et al. 1983; Sinclair et al. 1983). Moreover, deletion of all variant *H3.3* gene copies in
379 mouse embryonic fibroblasts results in disruption of heterochromatin domains at
380 pericentromeric repeat regions, centromeres, and telomeres (Jang et al. 2015).
381 Collectively, these findings indicate that *H3.2* and *H3.3* gene copy number play an
382 important role in establishing efficient silencing via H3K9me₃- and H3K27me₃-mediated
383 heterochromatin. We discuss below potential mechanisms for how changes in histone
384 gene copy number might impact Polycomb-mediated repressive chromatin.

385 ***Histone protein abundance and stoichiometry may influence Polycomb-mediated*** 386 ***repressive chromatin***

387 Here we show that although *12xHWT* animals develop normally, reducing *Pc* gene dose
388 by half in a *12xHWT* background results in mutant phenotypes associated with impaired
389 Polycomb-mediated gene silencing. This genetic interaction suggests that the
390 combination of reduced amounts of canonical histones and Polycomb prevents the proper

391 formation of a repressive chromatin domain at Polycomb-silenced genes. However, our
392 previous work found that canonical histone transcript levels are similar in *12xHWT* and
393 *200xWT* animals, at least in early embryos (11), and here we found similar levels of total
394 H3.3 and H3 protein in *12xHWT* and *200xWT* animals by western blotting. H3.2 and H3.3
395 are highly abundant proteins, and western blots may not provide the sensitivity needed
396 to identify small changes in H3 protein levels that could be biologically meaningful.
397 Moreover, a subtle decrease in histone protein abundance may result in changes in
398 nucleosome occupancy that preferentially affect heterochromatin function. Polycomb
399 chromatin domains have elevated nucleosome occupancy and decreased nucleosomal
400 spacing and therefore may be particularly sensitive to changes in histone abundance
401 (King et al. 2018). In fact, disruption of PRC1-mediated chromatin compaction in *D.*
402 *melanogaster* results in de-repression of Hox genes (Bonnet et al. 2022). In addition to
403 direct effects of decreased histone abundance at Polycomb target genes, it is also
404 possible that indirect effects contribute to Polycomb target gene misregulation in *12xHWT*
405 animals. Previous work showed that reductions in the concentration of free histone H3
406 results in increased local histone recycling during replication in *Xenopus* egg extracts and
407 *D. melanogaster* embryogenesis (Gruszka et al. 2020; Mühlen et al. 2023b). Thus,
408 another possibility is that reduced histone gene copy number results in an increased
409 proportion of recycled histones within chromatin. If recycled histones carry PTMs that
410 antagonize Polycomb function, such as H3K36me3, they could alter the PTM landscape
411 and impact target gene repression at Polycomb domains (Finogenova et al. 2020; Bonnet
412 et al. 2022; Mühlen et al. 2023b; Salzler et al. 2023). Future studies examining chromatin
413 accessibility and the PTM landscape at Polycomb target domains upon reduction in *H3*
414 gene copy number would help address these issues.

415 Nucleosomes and histone-chaperone complexes are multiprotein complexes that
416 assemble with defined stoichiometries (Luger et al. 1997; Andrews and Luger 2011;
417 Grover et al. 2018), and many genomic processes are sensitive to perturbations in subunit
418 stoichiometry within these complexes. For instance, disrupting the stoichiometric balance
419 between H2A:H2B dimers and H3:H4 dimers in yeast causes genome instability and
420 mitotic chromosome loss (Meeks-Wagner and Hartwell 1986). In all of the genotypes we
421 assessed that display mutant phenotypes indicative of impaired Polycomb repression, the
422 balance between *H3.2* and *H3.3* gene copy number is altered, and this change in the
423 relative abundance of H3.2 and H3.3 could impact genome regulation. Consistent with
424 this interpretation, work done in mice shows that displacement of H3.3—and enrichment
425 of replication dependent H3.1—at regulatory regions causes transcriptional deregulation
426 and chromosomal aberrations (Chen et al. 2020). Thus, the stoichiometric balance
427 between H3.2 and H3.3 in chromatin may be critical for maintaining Polycomb target gene
428 silencing in flies.

429 A corollary to this model is that proper stoichiometric balance between H3 proteins
430 and their chaperones is needed for repression of Polycomb targets. Previous work in
431 mouse cells shows that H3.3-specific chaperones interact with PRC1 and PRC2, and that
432 these interactions are needed for the recruitment of H3.3 to H3K9me3-dependent
433 heterochromatin and for the establishment of H3K27me3 at developmental gene
434 promoters (Banaszynski et al. 2013; Liu et al. 2020). Therefore, one could posit that
435 altering the stoichiometric balance between H3.3 and its chaperones may perturb the
436 establishment or maintenance of Polycomb domains. Notably, in our genetic screen for

437 viability we identified a deficiency that covers *Yem*, an H3.3-specific chaperone,
438 suggesting that mechanisms regulating the levels of canonical and variant histone within
439 the genome involve control of histone deposition into chromatin.

440 ***Distinct roles of canonical H3.2 and variant H3.3 in Polycomb-mediated silencing***

441 Canonical *H3.2* and variant *H3.3* differ in their expression patterns and protein sequence.
442 Our genetic analyses demonstrate that reducing *H3.3* gene copy number, but not *H3.2*
443 gene copy number, causes a decrease in viability of *Pc* heterozygotes, suggesting *H3.2*
444 and *H3.3* may have non-identical roles in Polycomb target gene regulation. *H3.3^A* mutants
445 do not uncouple *H3.2* expression from S phase, and *12xHWT* mutants still express *H3.3*
446 throughout all of interphase. Thus, depleting the pool of H3 outside of S phase in the
447 *H3.3^A* mutants may sensitize cells to small perturbations in Polycomb-mediated silencing
448 during development. For example, Polycomb Response Elements (PREs), such as those
449 that regulate *Ubx*, are sites of high histone turnover even though they reside within silent
450 chromatin domains (Mito et al. 2007). As such, PREs may be particularly sensitive to the
451 loss of available H3 protein outside of S phase. Reduced histone occupancy at PREs
452 could impact Polycomb repression and organismal viability. Our finding that viability of
453 animals with reduced *H3.2* gene copies increases as *H3.3* gene copy number increases
454 supports this model. Alternatively, canonical H3.2 and variant H3.3 proteins may have
455 distinct functions at PREs or Polycomb target domains. H3.2 and H3.3 differ at residue
456 31 on the N-terminal tail and H3.3S31 can be phosphorylated (H3.3S31ph). It is known
457 that histone H3 post-translational modifications can influence one another (Yuan et al.
458 2011; Finogenova et al. 2020). Notably, H3.3S31ph affects the local PTM landscape and
459 binding of factors that interact with the H3 tail, like the H3K36me3 reader ZMYND11
460 (Armache et al. 2020; Sitbon et al. 2020). Conceivably, these H3.3S31ph-specific effects
461 on the PTM landscape could impact Polycomb function. Future studies probing the
462 impacts of an H3.3S31A mutation, which renders the residue non-modifiable, on
463 Polycomb function would address this possibility.

464 In summary, our data investigating the control of canonical and variant histone
465 abundance provide evidence that Polycomb-mediated gene silencing is sensitive to both
466 canonical and variant histone gene copy number. This work advances our understanding
467 of the distinct and overlapping functions of canonical and variant histones.

468 **Tables**

Number ^a	Deficiency	Start coordinate ^b	End coordinate ^b	p value ^c
27	<i>Df(3L)BSC289</i>	1332329	1628100	-
45	<i>Df(3L)ED4287</i>	1795442	2551761	-
79	<i>Df(3L)ED4284</i>	1795442	1963552	-
80	<i>Df(3L)BSC385</i>	2259731	2417382	-
38	<i>Df(3L)BSC730</i>	12156077	12836424	-
51	<i>Df(3L)ED4606</i>	16080584	16773223	-
43	<i>Df(3L)BSC220</i>	18965662	19164368	-

Histone gene number impacts Polycomb

12

77	<i>Asf1[1]</i>	19619559	19619559	-
78	<i>E2F[rM729]</i>	21626545	21626545	-
82	<i>Df(3R)BSC527</i>	22626930	23111808	+
71	<i>Df(3R)ED6220</i>	24543798	25183773	-
73	<i>Df(3R)10-65</i>	81F	81F	-
76	<i>Df(3R)XNP[1]</i>	25477868	25482834	-
81 [♦]	<i>Df(3R)ro80b</i>	97D1	97D13	+
75	<i>Df(3R)BSC460</i>	27937830	28461658	-
83	<i>Df(3R)Exel6210</i>	28674961	28991018	+
66 [♦]	<i>Df(3R)BSC874</i>	28675029	29191671	++
70	<i>Df(3R)BSC789</i>	28820134	29040507	-
67	<i>Df(3R)BSC500</i>	29112527	29675700	++
68	<i>Df(3R)BSC501</i>	29112527	29724685	+
72	<i>Df(3R)ED6310</i>	29138895	29512153	-
74	<i>Stg[4]</i>	29252826	29255800	-
69	<i>Df(3R)BSC547</i>	29621303	29821399	-
<p>^a ♦ suggested haploinsufficiency</p> <p>^b Breakpoints are as determined by the Bloomington stock center.</p> <p>^c +, <i>p</i>-value < 0.05; ++, <i>p</i>-value < 0.01. <i>P</i>-values obtained from a Chi-square test.</p>				

469

Table 2. Chromosome 3L deficiency alleles tested for changes in viability.

Number ^a	Deficiency	Start coordinate ^b	End coordinate ^b	<i>p</i> value ^c
54	<i>Df(3L)ED50002</i>	22947	128631	-
23	<i>Df(3L)BSC362</i>	306168	628171	-
59	<i>Df(3L)Exel6085</i>	548528	749210	-
1 [♦]	<i>Df(3L)ED4196</i>	639583	1478937	++
27	<i>Df(3L)BSC289</i>	1332329	1628100	-
41	<i>Df(3L)BSC800</i>	1628101	1647451	-
46	<i>Df(3L)BSC181</i>	1688724	1841694	-
64	<i>Df(3L)Aprt-32</i>	1795318	2555775	+
45	<i>Df(3L)ED4287</i>	1795442	2551761	-
22	<i>Df(3L)BSC119</i>	2600282	2823614	-
35	<i>Df(3L)Exel6092</i>	2821245	3047162	-
32	<i>Df(3L)BSC671</i>	2982129	3193143	-
14	<i>Df(3L)BSC672</i>	3081311	3206906	-
37	<i>Df(3L)ED4293</i>	3226338	3250564	-
60	<i>Df(3L)BSC368</i>	3759821	4040635	-
55	<i>Df(3L)BSC884</i>	5601375	5770185	-
34	<i>Df(3L)BSC410</i>	5763773	6483285	-
39	<i>Df(3L)BSC411</i>	5969060	6618726	-

Histone gene number impacts Polycomb

13

19	<i>Df(3L)Exel6109</i>	6736213	6936639	-
53	<i>Df(3L)BSC27</i>	6936605	7136086	-
58	<i>Df(3L)BSC224</i>	6957557	7150109	-
50	<i>Df(3L)BSC33</i>	7242439	7350373	-
21	<i>Df(3L)BSC117</i>	7242575	7328086	-
30	<i>Df(3L)Exel8104</i>	7353086	7522363	-
13	<i>Df(3L)BSC375</i>	7510880	7904179	+
12	<i>Df(3L)BSC388</i>	7643513	8184286	-
63	<i>Df(3L)Exel6112</i>	8089573	8351924	-
56	<i>Df(3L)BSC815</i>	8256164	8499740	-
11	<i>Df(3L)BSC389</i>	8415284	8582696	+
16	<i>Df(3L)BSC816</i>	8632181	8738462	-
24	<i>Df(3L)ED4421</i>	8738426	9377175	-
47	<i>Df(3L)BSC113</i>	9342609	9416591	-
65	<i>Df(3L)AC1</i>	9351951	10140553	+
17	<i>Df(3L)BSC391</i>	9446770	9697191	-
26	<i>Df(3L)BSC118</i>	9508772	9690291	-
44	<i>Df(3L)BSC392</i>	9671802	9892354	-
15*	<i>Df(3L)BSC673</i>	9756714	10174058	+
48	<i>Df(3L)BSC439</i>	10507047	10964106	-
20	<i>Df(3L)ED4470</i>	11090089	11826330	-
49	<i>Df(3L)ED4475</i>	11580140	12401701	-
38	<i>Df(3L)BSC730</i>	12156077	12836424	-
25	<i>Df(3L)BSC12</i>	13037536	13221789	-
18	<i>Df(3L)ED4543</i>	13928325	14751140	-
33	<i>Df(3L)BSC845</i>	15504128	15819023	-
51	<i>Df(3L)ED4606</i>	16080584	16773223	-
6	<i>Df(3L)ED4674</i>	16654384	17042518	+
7	<i>Df(3L)BSC414</i>	16962973	17469226	+
62	<i>Df(3L)Exel6132</i>	17414682	17526191	-
57	<i>Df(3L)ED4710</i>	17487463	18139299	-
5	<i>Df(3L)BSC775</i>	17788244	18891426	+
43	<i>Df(3L)BSC220</i>	18965662	19164368	-
8*	<i>Df(3L)BSC839</i>	20313247	20486308	+
10	<i>Df(3L)BSC797</i>	20445923	20942833	-
31	<i>Df(3L)BSC449</i>	20850015	21196030	-
40	<i>Df(3L)BSC553</i>	20984731	21219092	-
3	<i>Df(3L)BSC419</i>	21218032	21597878	++
2	<i>Df(3L)BSC435</i>	21304739	21770618	++

36	<i>Df(3L)BSC836</i>	21382499	21497772	-
52	<i>Df(3L)BSC418</i>	21382499	21637924	-
9	<i>Df(3L)BSC223</i>	21909520	22078536	-
4 ^a	<i>Df(3L)BSC451</i>	22069194	22684788	++
42	<i>Df(3L)ED230</i>	22127751	22827471	-
29	<i>Df(3L)ED5017</i>	22828597	22991401	-
61	<i>Df(3L)1-16</i>	24292305	24536634	-
28	<i>Df(3L)6B-29</i>	24977118	25115180	-

^a ♦ suggested haploinsufficiency
^b Breakpoints are as determined by the Bloomington stock center.
^c +, p value < 0.05; ++, p value < 0.01. P-values obtained from a Chi-square test.

470

Table 3. Decrease in *H3.2* and *H3.3* gene copy number increases frequency of ectopic sex combs.

Genotype	# H3.3 genes	# H3.2 genes	% legs with ectopic sex combs ^a
<i>H3.3B^{+Y}; H3.3A^{+/+}, HisC^{+/+}; Df(3L)BSC419/+</i>	3	200	0%
<i>H3.3B^{+Y}; H3.3A^{+/-}, HisC^{+/-}; Df(3L)BSC419/12xHWT</i>	2	112	15% [•]
<i>H3.3B^{+Y}; H3.3A^{-/-}, HisC^{-/-}; Df(3L)BSC419/12xHWT</i>	1	12	40% [•]
<i>H3.3B^{+Y}; H3.3A^{-/-}, HisC^{-/-}; +/-12xHWT</i>	1	12	0%
<i>H3.3B^{+Y}; H3.3A^{+/-}, HisC^{+/-}; Pc³/12xHWT</i>	2	112	50% [▲]
<i>H3.3B^{+Y}; H3.3A^{-/-}, HisC^{-/-}; Pc³/12xHWT</i>	1	12	100% [▲]
<i>H3.3B^{+Y}; H3.3A^{+/+}, HisC^{-/-}; +/-12xHWT</i>	3	12	0%
<i>H3.3B^{+Y}; H3.3A^{+/+}, HisC^{+/-}; Pc³/12xHWT</i>	3	112	80% [■]
<i>H3.3B^{+Y}; H3.3A^{+/+}, HisC^{-/-}; Pc³/12xHWT</i>	3	12	100% ^{■†}
<i>H3.3B^{-Y}; H3.3A^{-/-}; HisC^{+/+};</i>	0	200	0%
<i>H3.3B^{+Y}; H3.3A^{+/+}, HisC^{+/+}; Pc³/+</i>	3	200	48%
<i>H3.3B^{+Y}; H3.3A^{+/-}, HisC^{+/+}; Pc³/+</i>	2	200	95% [*]
<i>H3.3B^{+Y}; H3.3A^{-/-}, HisC^{+/+}; Pc³/+</i>	1	200	96% [*]
<i>H3.3B^{-Y}; H3.3A^{-/-}, HisC^{+/+}; Pc³/+</i>	0	200	100% [*]

[•] Statistically significant difference in sex comb frequency between indicated genotype and *H3.3B^{+Y}; H3.3A^{+/+}, HisC^{+/+}; Df(3L)BSC419/+* (P-value < 0.0001).
[▲] Statistically significant difference in sex comb frequency between indicated genotype and *H3.3B^{+Y}; H3.3A^{-/-}, HisC^{-/-}; +/-12xHWT* (P-value < 0.0001).

▪ Statistically significant difference in sex comb frequency between indicated genotype and *H3.3B^{+Y}*; *H3.3A^{+/+}*, *HisC^{-/-}*; +12xHWT (*P*-value < 0.0001).
† Statistically significant difference in sex comb frequency between indicated genotype and *H3.3B^{+Y}*; *H3.3A^{+/+}*; *HisC^{+/-}*; *Pc³/12xHWT* (*P*-value < 0.0001).
* Statistically significant difference in sex comb frequency between indicated genotype and *H3.3B^{+Y}*; *H3.3A^{+/+}*, *HisC^{+/+}*; *Pc³/+* (*P*-value < 0.0001).
^a *P*-values obtained from a Fisher's exact test.

471

472 **Figures**

473 **Figure 1. *H3.3* is required for viability when *H3.2* gene copy number is reduced.** (A)
474 Diagram of the genomic locations of the three H3 genes and the 12xHWT transgene.
475 100x and 12x indicate gene copy number. (B) Schematic model of *H3.2* and *H3.3*
476 expression during the cell cycle. (C) Amino acid sequence differences of H3.2 and H3.3.
477 (D) Bar plot of viability for the indicated genotypes. Circles represent the full complement
478 of *H3.3* or *H3.2* gene copies present in the wild-type genome, and the color filling each
479 circle (*H3.3* green, *H3.2* blue) indicates the number of gene copies present in each
480 experimental genotype, e.g. a solid green circle indicates the 4 *H3.3* gene copies of the
481 diploid *H3.3A* and *H3.3B* loci. The number of *H3.2* genes is shown below the blue circles,
482 as well as whether surviving adults are fertile. Percent of expected genotypic frequencies
483 based on Mendelian ratios. Asterisks indicate fewer than expected survive (chi-square
484 test, ** *p* value < 0.01, see Figure 1 in File S1 for *p* values).

485 **Figure 2. *H3.3* mRNA and protein levels do not change when *H3.2* gene copy**
486 **number is reduced.** (A) MA plot showing fold change of normalized RNA-seq signal in
487 wild-type (200xWT) vs. 12xHWT for all transcripts (y-axis). Average coverage on the x-
488 axis represents the mean expression level of a transcript. Differentially expressed genes
489 are indicated in dark gray. Values for *H3.3A* and *H3.3B* transcripts are indicated (green).
490 (B) Western blot of total H3, H3.3 and tubulin from 12xHWT and 200xWT wandering third
491 instar larval wing imaginal discs. Dilution series with indicated number of wing discs for
492 each genotype. H3.3^A third instar larvae were used as a negative control. Bar plot
493 depicting the average fold change in H3.3 signal relative to 200xWT signal normalized to
494 tubulin. Error bars represent standard deviation of three biological replicates. (C) Confocal
495 images of third instar imaginal eye discs stained for DAPI (grey), EdU (magenta), and
496 H3.2 mRNA (cyan) for the four indicated genotypes, denoted as in Figure 1. The
497 maximum projection of four adjacent slices is shown. Bars, 50 μM.

498 **Figure 3. A genetic screen to identify genes required for survival when H3 gene**
499 **copy is reduced.** (A) Schematic of the screen used to identify regions of interest (ROI)
500 on chromosome 3 that when heterozygous or hemizygous reduce adult viability of the
501 *H3.3A^A*; 12xHWT experimental genotype compared to control siblings. H3 gene copy
502 number indicated as in Figure 1. Pink fill indicates gene copy number of the ROI. (B) Bar
503 plot of viability for 23 mutations on chr3L and chr3R (see Table 1). Asterisks indicate
504 statistical significance by Chi-square test (** *p* value < 0.01, * *p* value < 0.05, ♦ potential
505 haploinsufficiency irrespective of *H3* gene copy number, see Figure 3 in File S1 for *p*

506 values). Deficiencies covering region of interest indicated by orange bars. Data are
507 plotted as the percent of *H3.3A^A*; *12xHWT* animals inheriting the deficiency chromosome
508 relative to sibling animals inheriting the homologous balancer chromosome, which
509 establish the expected percentage (dashed line). (C) Diagram of deficiencies that
510 delineate a region of interest on chr3R from 98E5-99B9. The overlapping region specific
511 to the positive hits from 98F10-98F12 contains seven genes (green bar).

512 **Figure 4. Screen of chromosome 3L deficiencies identifies histone gene copy**
513 **number as a modifier of *Polycomb*.** (A) Bar plot of viability for 65 chr3L deficiency
514 mutations (see Table 2). Orange bars indicate two overlapping deficiencies that scored
515 positive and uncover the *Pc* locus. Data are plotted as in Figure 3. (B) Diagram of
516 deficiencies that delineate a region of interest on chr3L from 78C2-78F1. The overlapping
517 region specific to the positive hits from 78C6-78C8 contains nine genes (green bar).
518 *Df(3L)BSC435* (Df 2) and *Df(3L)BSC419* (Df 3) correspond to the orange bars in panel
519 A. (C) Bar plot of viability of *H3.3A^A*; *12xHWT* animals heterozygous for the seven
520 indicated mutations. Data are plotted as in Figure 3. Asterisks indicate statistical
521 significance by Chi-square test (** p value < 0.01, * p value < 0.05, ♦ potential
522 haploinsufficiency irrespective of *H3* gene copy number, see Figure 4 in File S1 for p
523 values).

524 **Figure 5. Reduced histone gene copy number disrupts *Polycomb* function.** (A)
525 Scanning electron micrographs of first (T1), second (T2), and third (T3) thoracic legs from
526 adult males of the indicated genotypes, depicted as in Figure 1 with *Pc* gene dose in pink.
527 Red brackets indicate the location where sex combs developed. (B) Confocal images of
528 wing imaginal discs of the indicated genotypes stained for DAPI (blue) and Ubx
529 (magenta). Red brackets indicate the wing pouch where ectopic Ubx expression
530 occurred. Bars, 50 μ M. (C) Bright field images of adult wings from the indicated
531 genotypes. (D) Bar plots of viability of *H3.3A^A*; *12xHWT* animals heterozygous for
532 mutations of PRC1 and PRC2 Polycomb complex members. Data are plotted as in Figure
533 3. Asterisks indicate statistical significance by Chi-square test (** p value < 0.01, ♦
534 potential haploinsufficiency irrespective of *H3* gene copy number, see Figure 5 in File S1
535 for p values).

536 **Figure 6. Polycomb function is sensitive to both *H3.2* and *H3.3* gene copy number.**
537 (A) Bar plot of viability for the indicated genotypes, depicted as in Figure 1 with *Pc* gene
538 dose in pink. Data are plotted as in Figure 3. Asterisks indicate statistical significance by
539 Chi-square test (** p value < 0.01, see Figure 6 in File S1 for p values). (B) Scanning
540 electron micrographs of first (T1), second (T2), and third (T3) thoracic legs from adult
541 males of the indicated genotypes. Red brackets indicate the location where sex combs
542 developed. (C) Confocal images of wing imaginal discs of the indicated genotypes stained
543 for DAPI (blue) and Ubx (magenta). Red brackets indicate the wing pouch where ectopic
544 Ubx expression occurred. Bars, 50 μ M. (D) Bright field images of adult wings of the
545 indicated genotypes.

546 **Materials & Methods**

547 **Fly Stocks & Husbandry:** Fly stocks were maintained on standard corn medium
548 provided by Archon Scientific (Durham, NC). See stocks in File S1 for a list of all stocks.

549 **CRISPR-mediated generation of $H3.3A^{\Delta}$:** pCFD4 plasmids encoding dual gRNAs
550 (gRNA_1: caaggcgccccgcaagcagc, gRNA_2: tgcaccgtgactatttcata) targeting $H3.3A$ were
551 injected into embryos expressing Cas9 from the *nanos* promoter (*y1 M{nos-Cas9.P}ZH-*
552 *2A w**; RRID: BDSC_54590) by *GenetiVision* Corporation (Houston, TX). $H3.3A^{\Delta}$ alleles
553 were identified by PCR of genomic DNA and confirmed by sequencing, which revealed a
554 265 bp deletion removing amino acids 19 through 94 of the $H3.3$ open reading frame.
555 The deletion breakpoints are indicated by ".../..." in the following sequence:
556 CAAGGCGCCCCGCA.../...TACGGTTCATGTAAT. The $H3.3A^{\Delta}$ allele was determined to
557 be amorphic because $H3.3B^0$; $H3.3A^{\Delta}$; $12xHWT/+$ animals are inviable.
558 CRISPR diagnostic screen primer set: $H3.3A^{\Delta}$ for-CCCGATGAATATAGGGTCACAC,
559 $H3.3A^{\Delta}$ rev-CTGGATGTCCTTGGGCATAAT. pCFD4-U6:1_U6:3 was a gift from Simon
560 Bullock (Addgene plasmid #49411; <http://n2t.net/addgene:49411>;
561 RRID:Addgene_49411). $H3.3A$ reference sequence: NCBI Gene ID 33736.

562 **Viability:** To examine the effect of $H3.2$ gene copy number on $H3.3^{null}$ viability (Figure
563 1D), the following four crosses were performed:

- 564 1. $H3.3B^0/H3.3B^0$; $H3.3A^{2x1}$, $\Delta HisC$, *twistGal4* / *CyO*; *x yw* / *Y*; $H3.3^{A2x1}$, $\Delta HisC$, *UAS-*
565 *YFP* / *CyO*; $12xHWT$ / $12xHWT$
- 566 2. $H3.3B^0/H3.3B^0$; $H3.3A^{2x1}$, $\Delta HisC$, *twistGal4* / *CyO*; *x yw* / *Y*; $H3.3^{A2x1}$, $\Delta HisC$, *UAS-*
567 *YFP* / *CyO*; $12xHWT-VK33$, $8xHWT-86F6$ / +
- 568 3. $H3.3B^0/H3.3B^0$; $H3.3A^{2x1}$, $\Delta HisC$, *twistGal4* / *CyO*; *x H3.3B^0* / *Y*; $H3.3A^{2x1}$ / *CyO*,
569 *twistGFP*
- 570 4. $H3.3B^0/H3.3B^0$; $H3.3A^{\Delta}$ / *CyO*, *twistGFP*; *x H3.3B^0* / *Y*; $H3.3A^{\Delta}$ / *CyO*, *twistGFP*;

571 To examine the effect of $H3.3$ gene copy number on $12xHWT$ viability (Figure 1D), the
572 following 3 crosses were performed:

- 573 1. $H3.3B^0/H3.3B^0$; $H3.3A^{2x1}$, $\Delta HisC$, *UAS-YFP* / *CyO*; $12xHWT$ / $12xHWT$ *x yw*;
574 $H3.3^{A2x1}$, *Df(2L) $\Delta HisC^{Cadillac}$* / *CyO*;
- 575 2. *yw* / *yw*; $H3.3A^{2x1}$, *Df(2L) $\Delta HisC^{Cadillac}$* ; $12xHWT$ / $12xHWT$ *x H3.3B^0* / *Y*; $H3.3A^{2x1}$,
576 $\Delta HisC$, *twistGal4* / *CyO*;
- 577 3. *yw* / *yw*; $\Delta HisC$, *twistGal4* / *CyO*; *x yw*; $\Delta HisC$, *UAS-YFP* / *CyO* ; $12xHWT$ /
578 $12xHWT$

579 Vials were maintained at 25°C and flipped every other day. Data were plotted as percent
580 observed of expected based on Mendelian ratios. Chi-squared analysis was performed
581 to determine statistical significance. A significance threshold of $p < 0.05$ was used in this
582 study. See stocks in File S1 for all genotypes and progeny numbers.

583 All genotypes were confirmed by PCR using the following primer sets:

Allele	Fwd primer (5' to 3')	Rev primer(s) (5' to 3')
<i>H3.3B⁰</i>	TAAGCATCTAGAATTTTCCTCTTGCTGC ACA	GCTGCCTCCGCGAATTA
<i>H3.3A^{2x1}</i>	GGGTCACACTGAGCAGACG	GATGTCCTTGGGCATAATGG
<i>H3.3A^Δ</i>	GGGTCACACTGAGCAGACG	GATGTCCTTGGGCATAATGG
<i>ΔHisC</i>	CCTGTGTTATATAAACCCGTGATA	GTGTCGCTTACGTTTCGTTAG
		CAATCATATCGCTGTCTCACTCA
<i>12xHWT</i>	CCTTCACGTTTTCCAGGT	CGACTGACGGTCGTAAGCAC
		AGTGTGTCGCTGTCGAGATG
<i>8xHWT</i>	TGACCTGTTCCGAGTGATTAG	AGGATGGGGGACAGAAGCAGCC

584

585 **RNA sequencing:** For each replicate sample, 25 brains were dissected from wandering
586 3rd instar larvae and homogenized in Trizol solution. RNA was isolated from the Trizol
587 aqueous phase using the Zymo RNA Clean and Concentrator-5 kit (Genesee Scientific
588 #11-352) including treatment with DNase I, as per the manufacturer's instructions.
589 Libraries were prepared from polyA selected RNA using the KAPA stranded mRNA kit
590 (Roche # 07962207001) and sequenced using the NOVASeq-S1 paired-end 100
591 platform. Sequence reads were trimmed for adaptor sequence/low-quality sequence
592 using BBDuk (bbmap v38.67) with parameters: ktrim=r, k=23, rcomp=t, tbo=t, tpe=t,
593 hdist=1, mink=11. Dm6 genome files for use with the STAR aligner were generated using
594 parameters: sjdbOverhang 99. Paired-end sequencing reads were aligned using STAR
595 v2.7.7a with default parameters (Dobin et al. 2013). featureCounts (subread v2.0.1) was
596 used with default parameters to count reads mapping to features (Liao et al. 2014).
597 DESeq2 (v1.34.0) was used to identify differentially expressed genes (Love et al. 2014).
598 Differentially expressed genes were defined as genes with an adjusted P-value less than
599 0.05 and an absolute log2 fold change greater than 1.

600 **Western blots:** Protein extracts from *H3.3^{null}* third instar larvae and *12xHWT* and *yw*
601 (*200xWT*) third instar larval wing discs were prepared by boiling samples for 10 minutes
602 in Laemmli SDS-PAGE loading buffer followed by sonication using the Bioruptor Pico
603 sonication system (Diagenode) for 10 cycles (30 sec on, 30 sec off). Samples were
604 clarified by centrifugation. Proteins were fractionated on BioRad Any kD™ Mini-
605 PROTEAN® TGX™ Precast Protein Gels GX (BioRad #4569033) and were transferred to
606 0.2um nitrocellulose membranes (BioRad #1620112) at 100V for 10 minutes and 60V for
607 20 minutes. Total protein was detected using G-Bioscience Swift Membrane Stain™ (G-
608 Bioscience, 786677). Membranes were probed using the following antibodies: rabbit anti-

609 H3 (1:60,000; Abcam Cat# ab1791, RRID:AB_302613), rabbit anti-H3.3 (1:1,000, Abcam
610 Cat# ab176840, RRID:AB_2715502), and mouse anti-tubulin (1:15,000, Sigma-Aldrich
611 Cat# T6074, RRID:AB_477582). Western blot analysis was performed using the following
612 HRP conjugated secondary antibodies: goat anti-Mouse-IgG-HRP (1:10,000, Thermo
613 Fisher Scientific Cat# 31430, RRID:AB_228307), donkey anti-Rabbit-IgG-HRP (1:10,000,
614 Cytiva Cat# NA934, RRID:AB_772206). Blots were detected using Amersham ECL
615 Prime Western blotting Detection Reagent (Cytiva, RPN2232). ImageLab densitometry
616 analysis was used to determine total protein, tubulin, H3.3, and H3 band intensity. Histone
617 signal was normalized to corresponding tubulin signal. Normalized signals from different
618 titrations of the same genotype were averaged and resulting values were set relative to
619 the wild-type value. This process was completed for three biological replicates. See
620 Figure in File S1 for raw data for each replicate.

621 **EdU + RNA FISH:** Third instar larval eye discs were dissected in Grace's medium and
622 incubated in 0.1 mg/mL EdU for 30 minutes. Samples were then washed in phosphate-
623 buffered saline (PBS) for 5 minutes, fixed for 30 minutes in 4% paraformaldehyde (16%
624 paraformaldehyde, diluted in PBS), washed 3x15 minutes in PBS with Triton (PBST)
625 (0.5% Triton X-100) and washed for 30 minutes in 3% Bovine serum albumin (BSA) in
626 PBS. EdU was detected using the Click-iT EdU Cy5 imaging kit (Invitrogen) according to
627 the manufacturer's instructions. After EdU detection, samples were washed in 3% BSA
628 for 15 minutes, washed in PBS for 5 minutes, and subsequently fixed in 4%
629 paraformaldehyde for 15 minutes. Next, RNA-FISH was performed using Stellaris® H3.2
630 mRNA probes with TAMRA fluorophores following the manufacturer's instructions for *D.*
631 *melanogaster* wing imaginal discs. Samples were stained with DAPI (1 ug/mL) at 37°C
632 for 30 minutes in Wash Buffer A. The maximum projection from 4 adjacent z-slices from
633 third instar wandering larval eye discs was used as representative images for each
634 genotype.

H3.2 RNA FISH probe set. Probes are oriented in the 3' to 5' direction.

acgttactacttcacgt	ttcacgcaaggccacggt	cgaagagaccaaccaggt
tctccgattgggttca	ctcttttgtagcgacga	ggcacacaagtggatc
gcagttgcttggtacga	tgcgattagaagctcgg	gtgacacgcttggcatga
ttccaccagtcgattgc	cagacgctggaaaggcag	ggatgtcttgggcatta
ccttagtagccagttgtt	tctgagcgatttcacgc	gccaatgcgtcgcgctaa
tggagcactcttgcgagc	atcgcaagtcctgcttaa	tcagcttaagcacgctcg
ttcttcacacctccggtg	cataaccgcccagctctg	atctgcaagttaatgccg
cagggcgatagcgggtggg	ttcgctagcttctgcag	atagagtacgctagcgt

635

636 **Genetic Screen Viability:** Bloomington third chromosome deficiency stock males were
637 crossed to *yw; H3.3A^{2x1}, ΔHisC, twistGal4 / CyO; MKRS / TM6B* virgin females.

638 Subsequently, *yw; H3.3A^{2x1}, ΔHisC, twistGal4 / +; Df(3) / MKRS* male progeny were
639 crossed with *yw; H3.3A^{2x1}, HisC^{Cadillac} / H3.3A^{2x1}, HisC^{Cadillac}; 12xHWT / 12xHWT* virgin
640 females. All fly stocks were maintained on standard corn medium at 25°C. Crosses were
641 flipped every other day for 8 days. Progeny were scored once per day. Animals eclosing
642 from deficiency crosses were counted beginning ten days post egg-laying based on the
643 presence or absence of dsRed from the *HisC^{Cadillac}* locus and stubble phenotype from
644 MKRS until all adult flies eclosed. Expected and observed ratios of the desired genotypes
645 were calculated following the completion of counting. Percent of expected was
646 determined by the ratio of *yw; H3.3A^{2x1}, ΔHisC, twistGal4 / H3.3A^{2x1}, Cadillac; Df(3) /*
647 *12xHWT* was to *yw; H3.3A^{2x1}, Cadillac / CyO ; Df(3) / 12xHWT* siblings. Significance was
648 determined by chi-square test; thresholds of $p < 0.05$ and $p < 0.01$ were used in this study.
649 All genotypes and progeny numbers can be found in File S1.

650 **Immunofluorescence:** For Ubx staining of wing discs, third instar larval cuticles were
651 inverted and fixed in 4% paraformaldehyde in PBS for 20 minutes at room temperature.
652 Cuticles were washed for 1 h in PBST (0.15% Triton X-100). Mouse anti-UBX (1:30,
653 DSHB Cat# FP3.38, RRID:AB_10805300) was used overnight at 4°C. Goat anti-mouse
654 IgG secondary antibody (1:1000, Thermo Fisher Scientific Cat# A-11029, lot #161153,
655 RRID:AB_2534088) was used for 2 hours at room temperature. DNA was counterstained
656 with DAPI (0.2ug/mL) and the discs were mounted in Vectashield® (VWR, 101098-042)
657 mounting media and imaged on a Leica Confocal SP8.

658 **Scanning electron microscopy:** One- to four-day-old flies were dehydrated in ethanol
659 and images of legs were taken using a Hitachi TM4000Plus tabletop SEM microscope at
660 15 kV and 500x magnification.

661 **Data Availability** Strains are available upon request. Raw RNA-seq data were deposited
662 to Gene Expression Omnibus (GEO) under accession GSE228058. Additional
663 information is available from the corresponding authors upon request.

664 **Acknowledgements** The authors thank Aaron Crain for the generation of the
665 *Df(2L)ΔHisC^{Cadillac}* allele.

666 **Funding** JEM and RLA were supported in part by the National Institute of Health
667 predoctoral traineeships: NIGMS T32GM135128 and NIGMS T32GM007092,
668 respectively. LG was supported in part by a National Institute of Health administrative
669 supplement to support undergraduate summer research to grant R35GM12885 (to DJM).
670 This work was supported by the National Institute of Health grants R35GM136435 (to
671 AGM), R35GM145258 (to RJD), R35GM128851 (to DJM).

672 **Conflict of Interest** None declared.

673 **References**

674 Loyola A, Almouzni G. 2007. Marking histone H3 variants: how, when and why? Trends
675 Biochem Sci. 32(9):425–433. doi:10.1016/J.TIBS.2007.08.004.

- 676 Ahmad K, Henikoff S. 2002. The histone variant H3.3 marks active chromatin by
677 replication-independent nucleosome assembly. *Mol Cell*. 9(6):1191–1200.
678 doi:10.1016/S1097-2765(02)00542-7.
- 679 Gossett AJ, Lieb JD. 2012. In vivo effects of histone H3 depletion on nucleosome
680 occupancy and position in *Saccharomyces cerevisiae*. *PLoS Genet*. 8(6).
681 doi:10.1371/JOURNAL.PGEN.1002771.
- 682 Allis CD JT& RD. 2007. *Epigenetics*. Second. Cold Spring Harbor Laboratory Press.
- 683 Andrews AJ, Luger K. 2011. Nucleosome Structure(s) and Stability: Variations on a
684 Theme. <http://dx.doi.org/10.1146/annurev-biophys-042910-155329>. 40(1):99–117.
685 doi:10.1146/ANNUREV-BIOPHYS-042910-155329.
- 686 Armache A, Yang S, Martínez de Paz A, Robbins LE, Durmaz C, Cheong JQ,
687 Ravishankar A, Daman AW, Ahimovic DJ, Klevorn T, et al. 2020. Histone H3.3
688 phosphorylation amplifies stimulation-induced transcription. *Nature*. 583(7818):852–
689 857. doi:10.1038/S41586-020-2533-0.
- 690 Armache A, Yang S, Robbins LE, Durmaz C, Daman AW, Jeong JQ, Paz AM de,
691 Ravishankar A, Arslan T, Lin S, et al. 2019. Phosphorylation of the ancestral histone
692 variant H3.3 amplifies stimulation-induced transcription. *bioRxiv*:.808048.
693 doi:10.1101/808048.
- 694 Bajusz I, Sipos L, Györgypál Z, Carrington EA, Jones RS, Gausz J, Gyurkovics H. 2001.
695 The Trithorax-mimic Allele of Enhancer of zeste Renders Active Domains of Target
696 Genes Accessible to Polycomb-Group-Dependent Silencing in *Drosophila*
697 *melanogaster*. *Genetics*. 159(3):1135–1150. doi:10.1093/GENETICS/159.3.1135.
- 698 Banaszynski LA, Wen D, Dewell S, Whitcomb SJ, Lin M, Diaz N, Elsässer SJ, Chappier
699 A, Goldberg AD, Canaani E, et al. 2013. Hira-dependent histone H3.3 deposition
700 facilitates prc2 recruitment at developmental loci in ES cells. *Cell*. 155(1):107–120.
701 doi:10.1016/j.cell.2013.08.061.
- 702 Berloco M, Fanti L, Breiling A, Orlando V, Pimpinelli S. 2001. The maternal effect gene,
703 abnormal oocyte (*abo*), of *Drosophila melanogaster* encodes a specific negative
704 regulator of histones. *Proc Natl Acad Sci U S A*. 98(21):12126–12131.
705 doi:10.1073/pnas.211428798.
- 706 Blackledge NP, Klose RJ. 2021. The molecular principles of gene regulation by
707 Polycomb repressive complexes. *Nature Reviews Molecular Cell Biology* 2021 22:12.
708 22(12):815–833. doi:10.1038/s41580-021-00398-y.
- 709 Bonnet J, Boichenko I, Kalb R, le Jeune M, Maltseva S, Pieropan M, Finkl K, Fierz B,
710 Müller J. 2022. PR-DUB preserves Polycomb repression by preventing excessive
711 accumulation of H2Aub1, an antagonist of chromatin compaction.
712 doi:10.1101/gad.350014.122.

- 713 Brown DT, Wellman SE, Sittman DB. 1985. Changes in the levels of three different
714 classes of histone mRNA during murine erythroleukemia cell differentiation. *Mol Cell*
715 *Biol.* 5(11):2879–2886. doi:10.1128/mcb.5.11.2879.
- 716 Bulchand S, Menon SD, George SE, Chia W. 2010. Muscle wasted: a novel component
717 of the *Drosophila* histone locus body required for muscle integrity. *J Cell Sci.*
718 123(16):2697–2707. doi:10.1242/JCS.063172.
- 719 Chen D, Chen QY, Wang Z, Zhu Y, Kluz T, Tan W, Li J, Wu F, Fang L, Zhang X, et al.
720 2020. Polyadenylation of Histone H3.1 mRNA Promotes Cell Transformation by
721 Displacing H3.3 from Gene Regulatory Elements. *iScience.* 23(9):101518.
722 doi:10.1016/J.ISCI.2020.101518.
- 723 Clark-Adams CD, Norris D, Osley MA, Fassler JS, Winston F. 1988. Changes in histone
724 gene dosage alter transcription in yeast. *Genes Dev.* 2(2):150–159.
725 doi:10.1101/gad.2.2.150.
- 726 Cook RK, Christensen SJ, Deal JA, Coburn RA, Deal ME, Gresens JM, Kaufman TC,
727 Cook KR. 2012. The generation of chromosomal deletions to provide extensive
728 coverage and subdivision of the *Drosophila melanogaster* genome. *Genome Biology*
729 2012 13:3. 13(3):1–14. doi:10.1186/GB-2012-13-3-R21.
- 730 Dobin A, Davis CA, Schlesinger F, Drenkow J, Zaleski C, Jha S, Batut P, Chaisson M,
731 Gingeras TR. 2013. STAR: ultrafast universal RNA-seq aligner. *Bioinformatics.*
732 29(1):15. doi:10.1093/BIOINFORMATICS/BTS635.
- 733 Duronio RJ, Marzluff WF. 2017. Coordinating cell cycle-regulated histone gene
734 expression through assembly and function of the Histone Locus Body. *RNA Biol.*
735 14(6):726–738. doi:10.1080/15476286.2016.1265198.
- 736 Eriksson PR, Ganguli D, Nagarajavel V, Clark DJ. 2012. Regulation of Histone Gene
737 Expression in Budding Yeast. doi:10.1534/genetics.112.140145.
- 738 Finogenova K, Bonnet J, Poepsel S, Schäfer IB, Finkl K, Schmid K, Litz C, Strauss M,
739 Benda C, Müller J. 2020. Structural basis for PRC2 decoding of active histone
740 methylation marks H3K36me2/3. *Elife.* 9:1–30. doi:10.7554/ELIFE.61964.
- 741 Goldberg AD, Banaszynski LA, Noh KM, Lewis PW, Elsaesser SJ, Stadler S, Dewell S,
742 Law M, Guo X, Li X, et al. 2010. Distinct Factors Control Histone Variant H3.3
743 Localization at Specific Genomic Regions. *Cell.* 140(5):678–691.
744 doi:10.1016/j.cell.2010.01.003.
- 745 Grover P, Asa JS, Campos EI. 2018. H3–H4 Histone Chaperone Pathways. *Annu Rev*
746 *Genet.* 52(1):109–130. doi:10.1146/annurev-genet-120417-031547.
- 747 Gruszka DT, Xie S, Kimura H, Yardimci H. 2020. Single-molecule imaging reveals
748 control of parental histone recycling by free histones during DNA replication. *Sci Adv.*
749 6(38):eabc0330. doi:10.1126/sciadv.abc0330.

- 750 Günesdogan U, Jäckle H, Herzig A. 2010. A genetic system to assess in vivo the
751 functions of histones and histone modifications in higher eukaryotes. *EMBO Rep.*
752 11:772–776. doi:10.1038/embor.2010.124.
- 753 Gunjan A, Verreault A. 2003. A Rad53 Kinase-Dependent Surveillance Mechanism that
754 Regulates Histone Protein Levels in *S. cerevisiae*. *Cell.* 115(5):537–549.
755 doi:10.1016/S0092-8674(03)00896-1.
- 756 Kaygun H, Marzluff WF. 2005. Regulated degradation of replication-dependent histone
757 mRNAs requires both ATR and Upf1. *Nat Struct Mol Biol.* 12(9):794–800.
758 doi:10.1038/NSMB972.
- 759 Hake SB, Garcia BA, Kauer M, Baker SP, Shabanowitz J, Hunt DF, Allis CD. 2005.
760 Serine 31 phosphorylation of histone variant H3.3 is specific to regions bordering
761 centromeres in metaphase chromosomes. *Proc Natl Acad Sci U S A.* 102(18):6344–
762 6349. doi:10.1073/pnas.0502413102.
- 763 Han M, Chang M, Kim UJ, Grunstein M. 1987. Histone H2B repression causes cell-
764 cycle-specific arrest in yeast: effects on chromosomal segregation, replication, and
765 transcription. *Cell.* 48(4):589–597. doi:10.1016/0092-8674(87)90237-6.
- 766 Harris ME, Böhni R, Schneiderman MH, Ramamurthy L, Schümperli D, Marzluff WF.
767 1991. Regulation of histone mRNA in the unperturbed cell cycle: evidence suggesting
768 control at two posttranscriptional steps. *Mol Cell Biol.* 11(5):2416–2424.
769 doi:10.1128/MCB.11.5.2416-2424.1991.
- 770 Hödl M, Basler K. 2012. Transcription in the absence of histone H3.2 and H3K4
771 methylation. *Current Biology.* 22(23):2253–2257. doi:10.1016/j.cub.2012.10.008.
- 772 Jang CW, Shibata Y, Starmer J, Yee D, Magnuson T. 2015. Histone H3.3 maintains
773 genome integrity during mammalian development. *Genes Dev.* 29(13):1377–1392.
774 doi:10.1101/gad.264150.115.
- 775 Kassis JA, Kennison JA, Tamkun JW. 2017. Polycomb and Trithorax Group Genes in
776 *Drosophila*. *Genetics.* 206(4):1699. doi:10.1534/GENETICS.115.185116.
- 777 Kaufman TC, Lewis R, Wakimoto B. 1980. Cytogenetic Analysis of Chromosome 3 in
778 *DROSOPHILA MELANOGASTER*: The Homoeotic Gene Complex in Polytene
779 Chromosome Interval 84a-B. *Genetics.* 94(1):115–133.
780 doi:10.1093/GENETICS/94.1.115.
- 781 Kennison JA, Tamkunt JW. 1988. Dosage-dependent modifiers of Polycomb and
782 Antennapedia mutations in *Drosophila*. *Proc Natl Acad Sci USA.* 85:8136–8140.
- 783 King HW, Fursova NA, Blackledge NP, Klose RJ. 2018. Polycomb repressive complex 1
784 shapes the nucleosome landscape but not accessibility at target genes. *Genome Res.*
785 28(10):1494–1507. doi:10.1101/GR.237180.118.

- 786 Kornberg RD, Lorch Y. 2020. Primary Role of the Nucleosome. *Mol Cell*. 79(3):371–
787 375. doi:10.1016/J.MOLCEL.2020.07.020.
- 788 Lewis PW, Elsaesser SJ, Noh K-M, Stadler SC, David Allis C. 2010. Daxx is an H3.3-
789 specific histone chaperone and cooperates with ATRX in replication-independent
790 chromatin assembly at telomeres. *National Acad Sciences*. 107.
791 doi:10.1073/pnas.1008850107/-/DCSupplemental.
- 792 Li Z, Johnson MR, Ke Z, Chen L, Welte MA. 2014. Drosophila lipid droplets buffer the
793 H2Av supply to protect early embryonic development. *Curr Biol*. 24(13):1485–1491.
794 doi:10.1016/J.CUB.2014.05.022.
- 795 Liao Y, Smyth GK, Shi W. 2014. featureCounts: an efficient general purpose program
796 for assigning sequence reads to genomic features. *Bioinformatics*. 30(7):923–930.
797 doi:10.1093/BIOINFORMATICS/BTT656.
- 798 Lifton RP, Goldberg ML, Karp RW, Hogness DS. 1977. The organization of the histone
799 genes in *Drosophila melanogaster*: Functional and evolutionary implications. *Cold
800 Spring Harb Symp Quant Biol*. 42(2):1047–1051. doi:10.1101/sqb.1978.042.01.105.
- 801 Liu Z, Tardat M, Gill ME, Royo H, Thierry R, Ozonov EA, Peters AH. 2020. SUMOylated
802 PRC1 controls histone H3.3 deposition and genome integrity of embryonic
803 heterochromatin. *EMBO J*. 39(13):e103697. doi:10.15252/EMBJ.2019103697.
- 804 Love MI, Huber W, Anders S. 2014. Moderated estimation of fold change and
805 dispersion for RNA-seq data with DESeq2. *Genome Biology* 2014 15:12. 15(12):1–21.
806 doi:10.1186/S13059-014-0550-8.
- 807 Luger K, Mäder A, Richmond R, Nature DS-, 1997 U. 1997. Crystal structure of the
808 nucleosome core particle at 2.8 Å resolution. *nature.com*.
- 809 Malik HS, Henikoff S. 2003. Phylogenomics of the nucleosome. *Nat Struct Biol*.
810 10(11):882–891. doi:10.1038/nsb996.
- 811 Martire S, Banaszynski LA. 2020 Jul 14. The roles of histone variants in fine-tuning
812 chromatin organization and function. *Nat Rev Mol Cell Biol*.:1–20. doi:10.1038/s41580-
813 020-0262-8.
- 814 Martire S, Gogate AA, Whitmill A, Tafessu A, Nguyen J, Teng YC, Tastemel M,
815 Banaszynski LA. 2019. Phosphorylation of histone H3.3 at serine 31 promotes p300
816 activity and enhancer acetylation. *Nat Genet*. 51(6):941–946. doi:10.1038/s41588-019-
817 0428-5.
- 818 Marzluff WF, Duronio RJ. 2002. Histone mRNA expression: Multiple levels of cell cycle
819 regulation and important developmental consequences. *Curr Opin Cell Biol*. 14(6):692–
820 699. doi:10.1016/S0955-0674(02)00387-3.

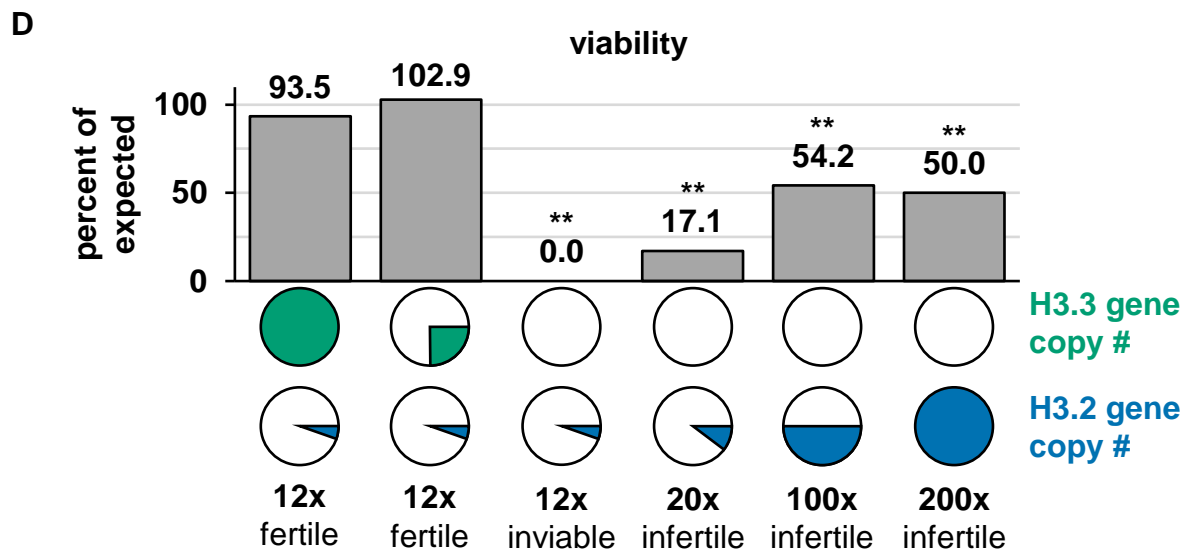
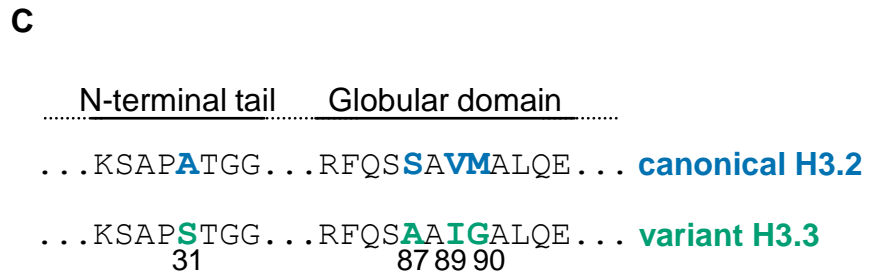
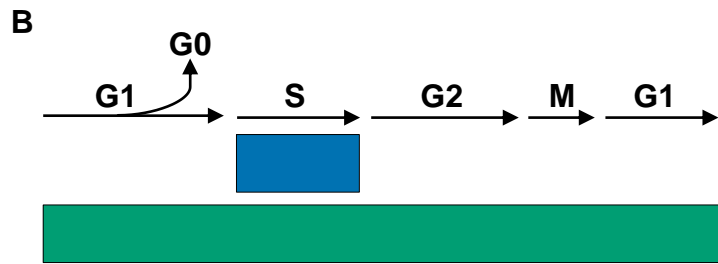
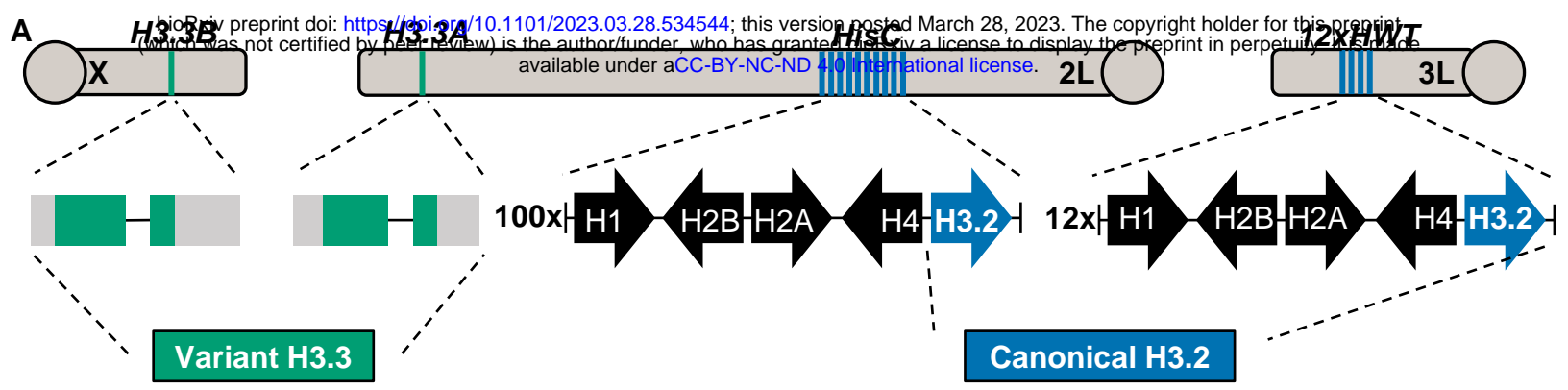
- 821 Marzluff WF, Gongidi P, Woods KR, Jin J, Maltais LJ. 2002a. The Human and Mouse
822 Replication-Dependent Histone Genes. *Genomics*. 80(5):487–498.
823 doi:10.1006/GENO.2002.6850.
- 824 Marzluff WF, Gongidi P, Woods KR, Jin J, Maltais LJ. 2002b. The Human and Mouse
825 Replication-Dependent Histone Genes. *Genomics*. 80(5):487–498.
826 doi:10.1006/GENO.2002.6850.
- 827 Maze I, Wenderski W, Noh K-M, Bagot RC, Tzavaras N, Purushothaman I, Elsässer SJ,
828 Guo Y, Ionete C, Hurd YL, et al. 2015. Critical role of histone turnover in neuronal
829 transcription and plasticity. *Neuron*. 87(1):77. doi:10.1016/J.NEURON.2015.06.014.
- 830 McKay DJ, Klusza S, Penke TJR, Meers MP, Curry KP, McDaniel SL, Malek PY,
831 Cooper SW, Tatomer DC, Lieb JD, et al. 2015. Interrogating the function of metazoan
832 histones using engineered gene clusters. *Dev Cell*. 32(3):373.
833 doi:10.1016/J.DEVCEL.2014.12.025.
- 834 McKittrick E, Gafken PR, Ahmad K, Henikoff S. 2004. Histone H3.3 is enriched in
835 covalent modifications associated with active chromatin. *Proc Natl Acad Sci U S A*.
836 101(6):1525–1530. doi:10.1073/pnas.0308092100.
- 837 Meeks-Wagner D, Hartwell LH. 1986. Normal stoichiometry of histone dimer sets is
838 necessary for high fidelity of mitotic chromosome transmission. *Cell*. 44(1):43–52.
839 doi:10.1016/0092-8674(86)90483-6.
- 840 Mito Y, Henikoff JG, Henikoff S. 2005. Genome-scale profiling of histone H3.3
841 replacement patterns. *Nat Genet*. 37(10):1090–1097. doi:10.1038/ng1637.
- 842 Mito Y, Henikoff JG, Henikoff S. 2007. Histone replacement marks the boundaries of
843 cis-regulatory domains. *Science* (1979). 315(5817):1408–1411.
844 doi:10.1126/science.1134004.
- 845 Smith MM, Murray K. 1983. Yeast H3 and H4 histone messenger RNAs are transcribed
846 from two non-allelic gene sets. *J Mol Biol*. 169(3):641–661. doi:10.1016/S0022-
847 2836(83)80163-6.
- 848 Moore GD, Procnier JD, Cross DP, Grigliatti TA. 1979. Histone gene deficiencies and
849 position–effect variegation in *Drosophila*. *Nature* 1979 282:5736. 282(5736):312–314.
850 doi:10.1038/282312a0.
- 851 Moore GD, Sinclair DA, Grigliatti TA. 1983. HISTONE GENE MULTIPLICITY AND
852 POSITION EFFECT VARIATION IN *DROSOPHILA MELANOGASTER*.
- 853 Mühlen D, Li X, Dovgusha O, Jäckle H, Günesdogan U. 2023a. Recycling of parental
854 histones preserves the epigenetic landscape during embryonic development. *Sci Adv*.
855 doi:10.1126/SCIADV.ADD6440.
- 856 Mühlen D, Li X, Dovgusha O, Jäckle H, Günesdogan U. 2023b. Recycling of parental
857 histones preserves the epigenetic landscape during embryonic development. *Sci Adv*.

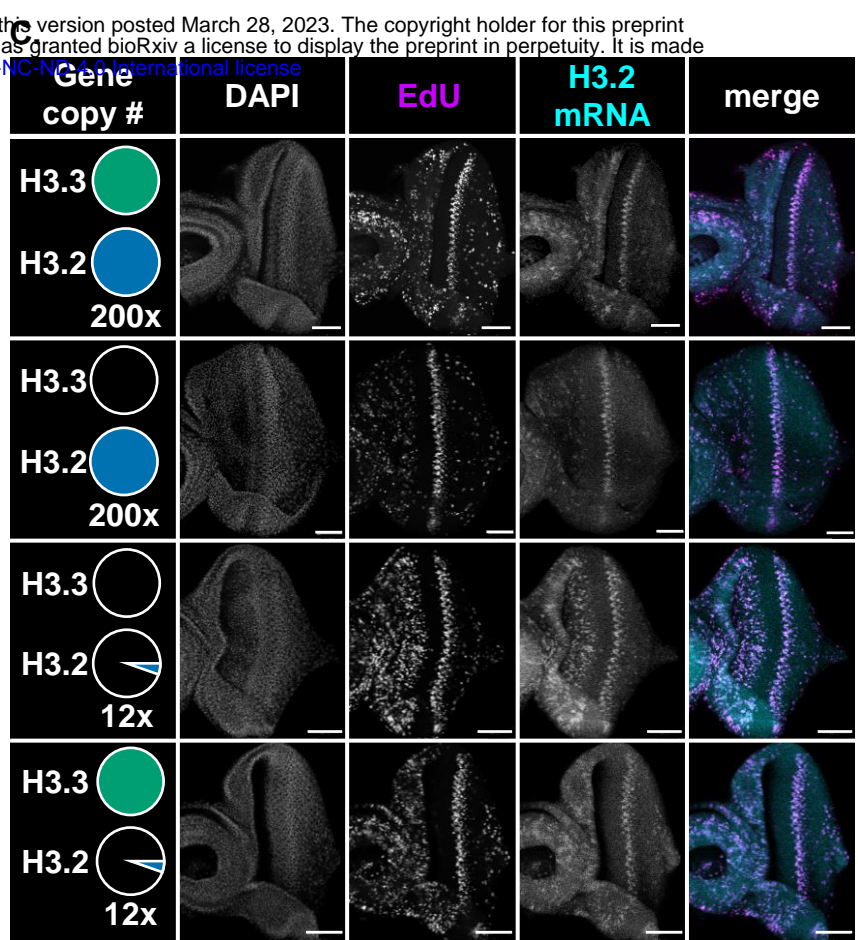
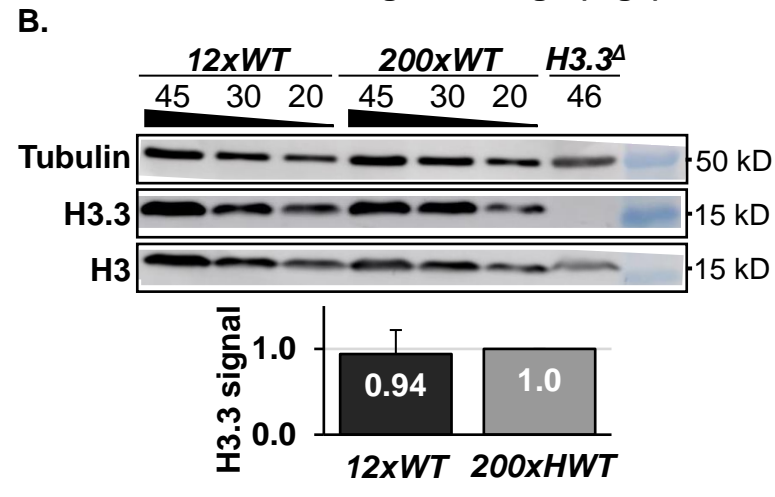
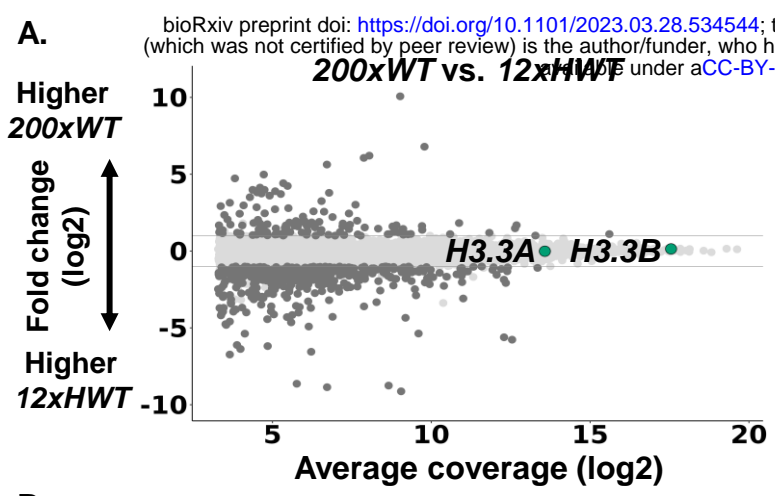
- 858 9(5):eadd6440.
859 doi:10.1126/SCIADV.ADD6440/SUPPL_FILE/SCIADV.ADD6440_SM.PDF.
- 860 Myung K, Pennaneach V, Kats ES, Kolodner RD. 2003. *Saccharomyces cerevisiae*
861 chromatin-assembly factors that act during DNA replication function in the maintenance
862 of genome stability. *Proc Natl Acad Sci U S A*. 100(11):6640–6645.
863 doi:10.1073/PNAS.1232239100.
- 864 Nashun B, Hill PWS, Smallwood SA, Dharmalingam G, Amouroux R, Clark SJ, Sharma
865 V, Ndjetehe E, Pelczar P, Festenstein RJ, et al. 2015. Continuous Histone Replacement
866 by Hira Is Essential for Normal Transcriptional Regulation and De Novo DNA
867 Methylation during Mouse Oogenesis. *Mol Cell*. 60(4):611–625.
868 doi:10.1016/j.molcel.2015.10.010.
- 869 Nelson DM, Ye X, Hall C, Santos H, Ma T, Kao GD, Yen TJ, Harper JW, Adams PD.
870 2002. Coupling of DNA Synthesis and Histone Synthesis in S Phase Independent of
871 Cyclin/cdk2 Activity. *Mol Cell Biol*. 22(21):7459. doi:10.1128/MCB.22.21.7459-
872 7472.2002.
- 873 Orlando V. 2003. Polycomb, epigenomes, and control of cell identity. *Cell*. 112(5):599–
874 606. doi:10.1016/S0092-8674(03)00157-0.
- 875 Orsi GA, Algazeery A, Meyer RE, Capri M, Sapey-Triomphe LM, Horard B, Gruffat H,
876 Couble P, Aït-Ahmed O, Loppin B. 2013. *Drosophila* Yemanuclein and HIRA Cooperate
877 for De Novo Assembly of H3.3-Containing Nucleosomes in the Male Pronucleus.
878 Ferguson-Smith AC, editor. *PLoS Genet*. 9(2):e1003285.
879 doi:10.1371/journal.pgen.1003285.
- 880 Pantazis P, Bonner WM. 1984. Specific alterations in the pattern of histone-3 synthesis
881 during conversion of human leukemic cells to terminally differentiated cells in culture.
882 *Differentiation*. 28(2):186–190. doi:10.1111/j.1432-0436.1984.tb00282.x.
- 883 Paro R. 1990. Imprinting a determined state into the chromatin of *Drosophila*. *Trends in*
884 *Genetics*. 6(C):416–421. doi:10.1016/0168-9525(90)90303-N.
- 885 Pattatucci AM, Otteson DC, Kaufman TC. 1991. A Functional and Structural Analysis of
886 the Sex Combs Reduced Locus of *Drosophila Melanogaster*. *Genetics*. 129(2):423.
887 doi:10.1093/GENETICS/129.2.423.
- 888 Piña B, Suau P. 1987. Changes in histones H2A and H3 variant composition in
889 differentiating and mature rat brain cortical neurons. *Dev Biol*. 123(1):51–58.
890 doi:10.1016/0012-1606(87)90426-X.
- 891 Eriksson PR, Ganguli D, Nagarajavel V, Clark DJ. 2012. Regulation of histone gene
892 expression in budding yeast. *Genetics*. 191(1):7–20.
893 doi:10.1534/GENETICS.112.140145.

- 894 Rai TS, Puri A, McBryan T, Hoffman J, Tang Y, Pchelintsev NA, Tuyn J van,
895 Marmorstein R, Schultz DC, Adams PD. 2011. Human CABIN1 Is a Functional Member
896 of the Human HIRA/UBN1/ASF1a Histone H3.3 Chaperone Complex. *Mol Cell Biol.*
897 31(19):4107. doi:10.1128/MCB.05546-11.
- 898 Ray-Gallet D, Ricketts M, Sato Y, ... KG-N, 2018 U. 2018. Functional activity of the H3.
899 3 histone chaperone complex HIRA requires trimerization of the HIRA subunit. *Nat*
900 *Commun.*
- 901 Roote J, Russell S. 2012. Toward a complete Drosophila deficiency kit. *Genome Biol.*
902 13(3):149. doi:10.1186/GB-2012-13-3-149.
- 903 Sakai A, Schwartz BE, Goldstein S, Ahmad K. 2009. Transcriptional and Developmental
904 Functions of the H3.3 Histone Variant in Drosophila. *Current Biology.* 19(21):1816–
905 1820. doi:10.1016/j.cub.2009.09.021.
- 906 Salzler HR, Vandadi V, McMichael BD, Brown JC, Boerma SA, Leatham-Jensen MP,
907 Adams KM, Meers MP, Simon JM, Duronio RJ, et al. 2023. Distinct roles for canonical
908 and variant histone H3 lysine-36 in Polycomb silencing. *Sci Adv.* 9(9).
909 doi:10.1126/SCIADV.ADF2451.
- 910 Sauer P, Gu Y, Liu WH, Mattioli F, Panne D, Luger K, Churchill M. 2018. Mechanistic
911 insights into histone deposition and nucleosome assembly by the chromatin assembly
912 factor-1. *Nucleic Acids Res.* 46(19):9907–9917. doi:10.1093/NAR/GKY823.
- 913 Schneiderman JI, Sakai A, Goldstein S, Ahmad K. 2009. The XNP remodeler targets
914 dynamic chromatin in Drosophila. *Proc Natl Acad Sci U S A.* 106(34):14472–14477.
915 doi:10.1073/pnas.0905816106.
- 916 Franklin S, Zweidler A. 1977. Non-allelic variants of histones 2a, 2b and 3 in mammals.
917 *Nature.* 266(5599):273–275. doi:10.1038/266273A0.
- 918 Shibahara KI, Stillman B. 1999. Replication-dependent marking of DNA by PCNA
919 facilitates CAF-1-coupled inheritance of chromatin. *Cell.* 96(4):575–585.
920 doi:10.1016/S0092-8674(00)80661-3.
- 921 Sinclair DAR, Mottus RC, Grigliatti TA. 1983. Genes which suppress position-effect
922 variegation in Drosophila melanogaster are clustered. *Molecular and General Genetics*
923 *MGG* 191:2. 191(2):326–333. doi:10.1007/BF00334834.
- 924 Singh RK, Kabbaj MHM, Paik J, Gunjan A. 2009. Histone levels are regulated by
925 phosphorylation and ubiquitylation-dependent proteolysis. *Nat Cell Biol.* 11(8):925–933.
926 doi:10.1038/NCB1903.
- 927 Sitbon D, Boyarchuk E, Dingli F, Loew D, Almouzni G. 2020. Histone variant H3.3
928 residue S31 is essential for Xenopus gastrulation regardless of the deposition pathway.
929 *Nat Commun.* 11(1):1–15. doi:10.1038/s41467-020-15084-4.

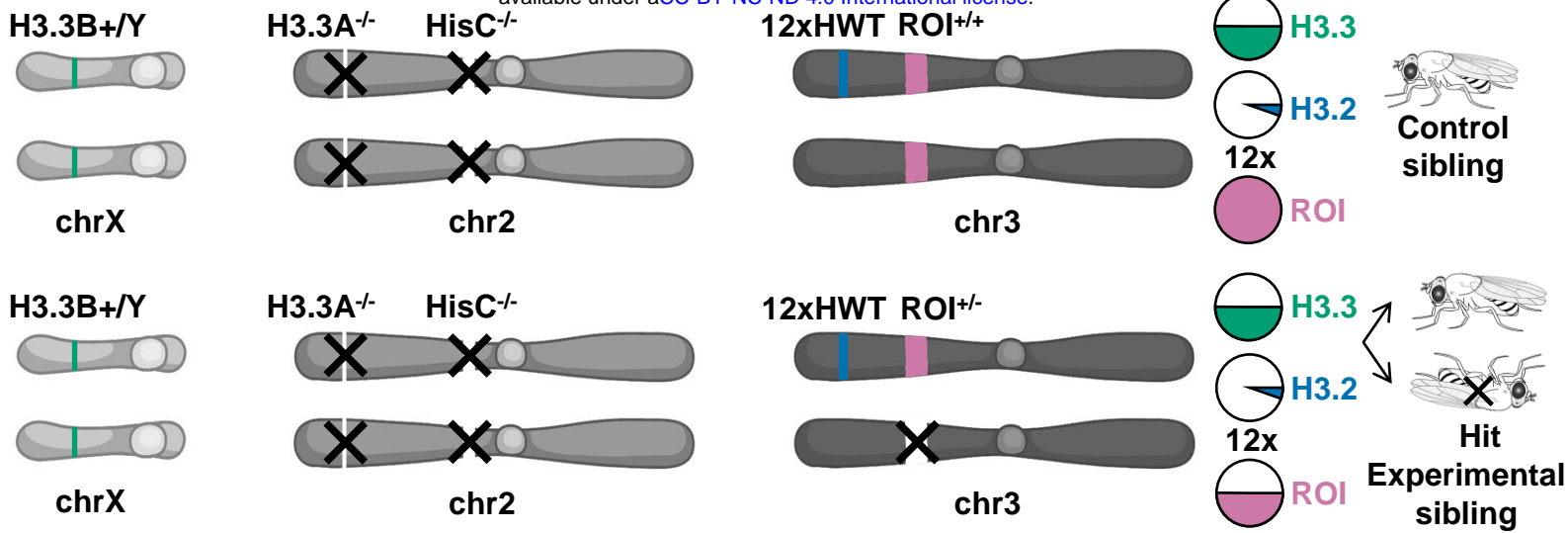
- 930 Smith A v., King JA, Orr-Weaver TL. 1993. Identification of genomic regions required for
931 DNA replication during *Drosophila* embryogenesis. *Genetics*. 135(3):817–829.
932 doi:10.1093/GENETICS/135.3.817.
- 933 Smith S, Stillman B. 1989. Purification and Characterization of CAF-I, a Human Cell
934 Factor Required for Chromatin Assembly during DNA Replication In Vitro.
- 935 Stephenson RA, Thomalla JM, Chen L, Kolkhof P, White RP, Beller M, Welte MA. 2021.
936 Sequestration to lipid droplets promotes histone availability by preventing turnover of
937 excess histones. *Development (Cambridge)*. 148(15).
938 doi:10.1242/DEV.199381/270998/AM/SEQUESTRATION-TO-LIPID-DROPLETS-
939 PROMOTES-HISTONE.
- 940 Sullivan E, Santiago C, Parker ED, Dominski Z, Yang X, Lanzotti DJ, Ingledue TC,
941 Marzluff WF, Duronio RJ. 2001. *Drosophila* stem loop binding protein coordinates
942 accumulation of mature histone mRNA with cell cycle progression. *Genes Dev*.
943 15(2):173–187. doi:10.1101/gad.862801.
- 944 Szenker E, Ray-Gallet D, Almouzni G. 2011. The double face of the histone variant
945 H3.3. *Cell Res*. 21(3):421–434. doi:10.1038/cr.2011.14.
- 946 Tagami H, Ray-Gallet D, Almouzni G, Nakatani Y. 2004. Histone H3.1 and H3.3
947 Complexes Mediate Nucleosome Assembly Pathways Dependent or Independent of
948 DNA Synthesis. *Cell*. 116(1):51–61. doi:10.1016/S0092-8674(03)01064-X.
- 949 Torné J, Ray-Gallet D, Boyarchuk E, Garnier M, le Baccon P, Coulon A, Orsi GA,
950 Almouzni G. 2020. Two HIRA-dependent pathways mediate H3.3 de novo deposition
951 and recycling during transcription. *Nature Structural & Molecular Biology* 2020 27:11.
952 27(11):1057–1068. doi:10.1038/s41594-020-0492-7.
- 953 Tvardovskiy A, Schwämmle V, Kempf SJ, Rogowska-Wrzesinska A, Jensen ON. 2017.
954 Accumulation of histone variant H3.3 with age is associated with profound changes in
955 the histone methylation landscape. *Nucleic Acids Res*. 45(16):9272–9289.
956 doi:10.1093/nar/gkx696.
- 957 Urban MK, Zweidler A. 1983. Changes in nucleosomal core histone variants during
958 chicken development and maturation. *Dev Biol*. 95(2):421–428. doi:10.1016/0012-
959 1606(83)90043-X.
- 960 Verreault A, Kaufman PD, Kobayashi R, Stillman B. 1996. Nucleosome assembly by a
961 complex of CAF-1 and acetylated histones H3/H4. *Cell*. 87(1):95–104.
962 doi:10.1016/S0092-8674(00)81326-4.
- 963 Wirbelauer C, Bell O, Schübeler D. 2005. Variant histone H3.3 is deposited at sites of
964 nucleosomal displacement throughout transcribed genes while active histone
965 modifications show a promoter-proximal bias. *Genes Dev*. 19(15):1761–1766.
966 doi:10.1101/gad.347705.

- 967 Wunsch AM, Lough J. 1987. Modulation of histone H3 variant synthesis during the
968 myoblast-myotube transition of chicken myogenesis. *Dev Biol.* 119(1):94–99.
969 doi:10.1016/0012-1606(87)90210-7.
- 970 Ye X, Franco AA, Santos H, Nelson DM, Kaufman PD, Adams PD. 2003. Defective S
971 phase chromatin assembly causes DNA damage, activation of the S phase checkpoint,
972 and S phase arrest. *Mol Cell.* 11(2):341–351. doi:10.1016/S1097-2765(03)00037-6.
- 973 Yuan W, Xu M, Huang C, Liu N, Chen S, Zhu B. 2011. H3K36 Methylation Antagonizes
974 PRC2-mediated H3K27 Methylation. *J Biol Chem.* 286(10):7983.
975 doi:10.1074/JBC.M110.194027.
- 976 Zweidler A. 1984. Core histone variants of the mouse: primary structure and differential
977 expression. Wiley New York.
- 978

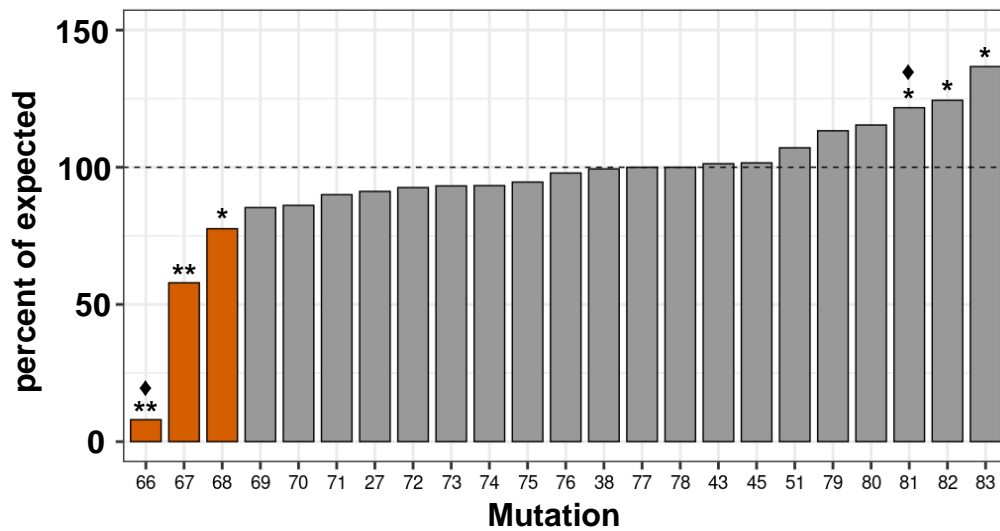




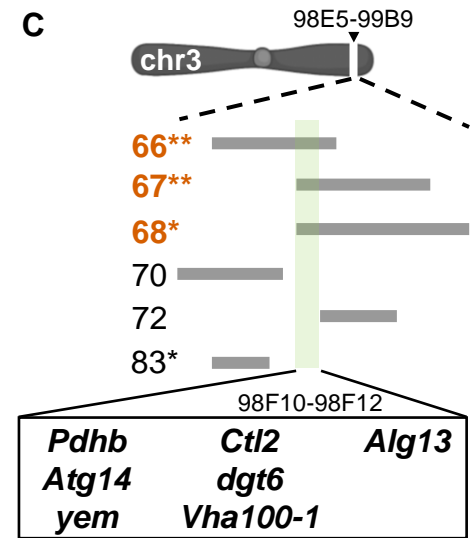
A



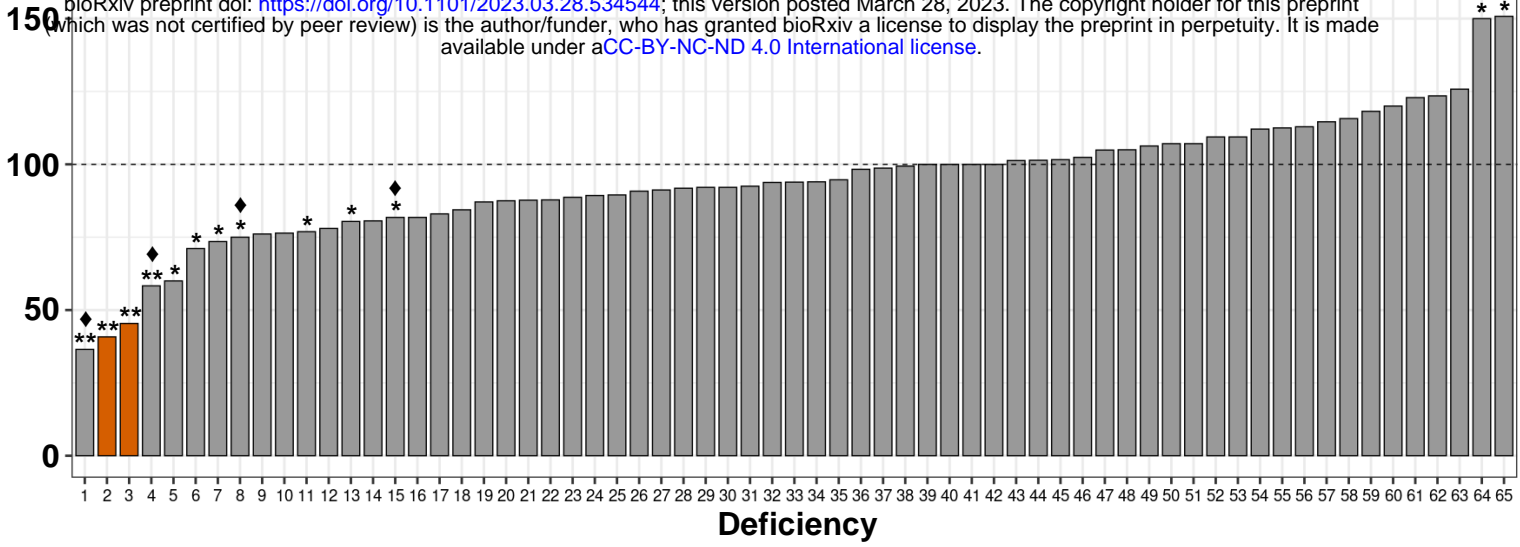
B



C

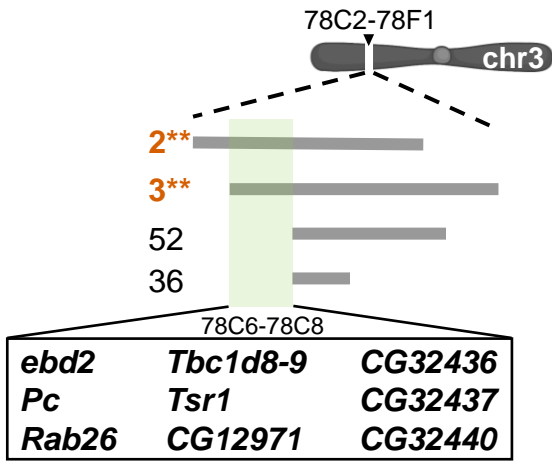


percent of expected



Deficiency

B



C

